The discrepancies in Fig. 6.9b between simulation and analysis probably stem from the particular treatment of the additive noise. In [Busch & Kaiser 2003], the noise term is included in the slow v-variable, while in the analytical model, noise is added to the fast activator variable u. Usually the location of the additive noise term in the FHN system is not essential for the output dynamics, because the fluctuations shift the relative positions of the null clines in a similar way. In the Barkley model, however, a noisy inhibitor variable also causes the fluctuations to enter the activator dynamics multiplicatively in u via the u_{thr}-function, possibly resulting in a different dynamical behavior.
It is indeed possible to continously shift from the band-pass to the low-pass response characteristics of the full spatiotemporal dynamics by continously varying the parameter r in the FitzHugh-Nagumo system. A change of r within certain bounds ($r_{\mathrm{thr}} \geq 0.0871$) still leaves the individual system in the excitable dynamical regime, while the system becomes bistable, if $r < r_{\mathrm{thr}}$. The excitability threshold changes with r, but as we are interested in the relative shift of the mutual information maximum with changing noise color τ, the results will still be comparable. The outcome of these investigations are depicted in Fig. 6.9b. Both the numerical and the analytical results are in good agreement. The function σ^2_{rel} becomes asymmetric with respect to τ for decreasing r. Eventually the analytical predictions would converge with the monotonous behavior found in the linear model of the Barkley system for $r = 0$.

6.1.2 Spatiotemporal Power-law Noise

The section investigates the influence of spatiotemporal power-law noise on STSR in a network of coupled FitzHugh Nagumo systems [Busch et al. 2003]. We expect different results as compared to the case of short-range, exponentially correlated noise, because of the spatiotemporal self-affine properties in the power-law noise.
The response of the sub-excitable medium towards pattern formation can be seen from Fig. 6.10. Similar to the results of the previous section, one finds optimal pattern formation for a finite noise level. Moreover, there is some intermediate temporal noise color $\alpha \approx 1.0$ for which σ^2_{opt} assumes a minimum. The behavior of pattern formation with respect to the spatial noise correlation is not immediately obvious. The system exhibits patchiness for all β, and in contrast to the previous case using short-ranged correlated noise, a large spatial noise color does not result in large synchronously spiking areas of the network. This behavior is explained from the spatiotemporal roughness of the power-law noise (cf. Figs. 2.2 and 2.7). A high spatial correlation of the noise does not necessarily cause nearest-neighbor noise values to be in the same favorable state due

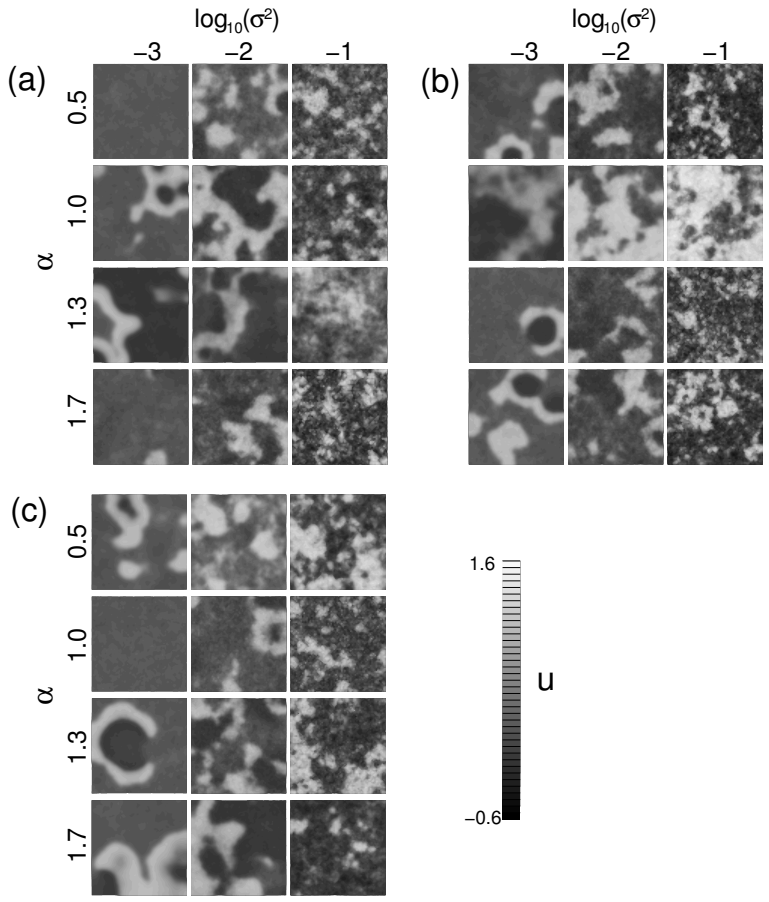

Figure 6.10: Snapshots of the network for various noise strengths σ^2 (columns) and temporal noise color (rows) for 3 values of spatial correlations. (a) $\beta = 0.5$ (b) $\beta = 1.0$, (c) $\beta = 1.5$. Shown are the u-variables of each grid point (Eq. 3.7). All snapshots have been taken after a transient of $50\,t.u.$. $N = 64$, $D_u = 0.2$. Other parameters: (ϵ,a,r,γ,b) = (0.005,0.5,1.0,1.0,0.21).

to the self-affine properties of the power-law noise.

A systematic investigation using both the mutual information I and the auto-covariance S elucidate the systematics of the noise-induced pattern formation under the influence of spatiotemporal power-law noise. Figure 6.11 shows both measures as a function of the noise intensity σ^2 and the temporal noise color τ. Similar to the exponentially correlated noise, the auto-covariance and the mutual information show a boomerang-shaped functionality with respect to the temporal noise color, minimizing the noise level for STSR around $\alpha \approx 1$. Furthermore, there is no such occurrence of a second maximum developing with increasing spatial noise color as seen previously in Fig. 6.4. This supports the visual impression, that the system remains patchy for all β.

The main difference between S and I in the interpretation of noise-induced structures becomes obvious from Fig. 6.12, which depicts the dependence of S and I on the spatial

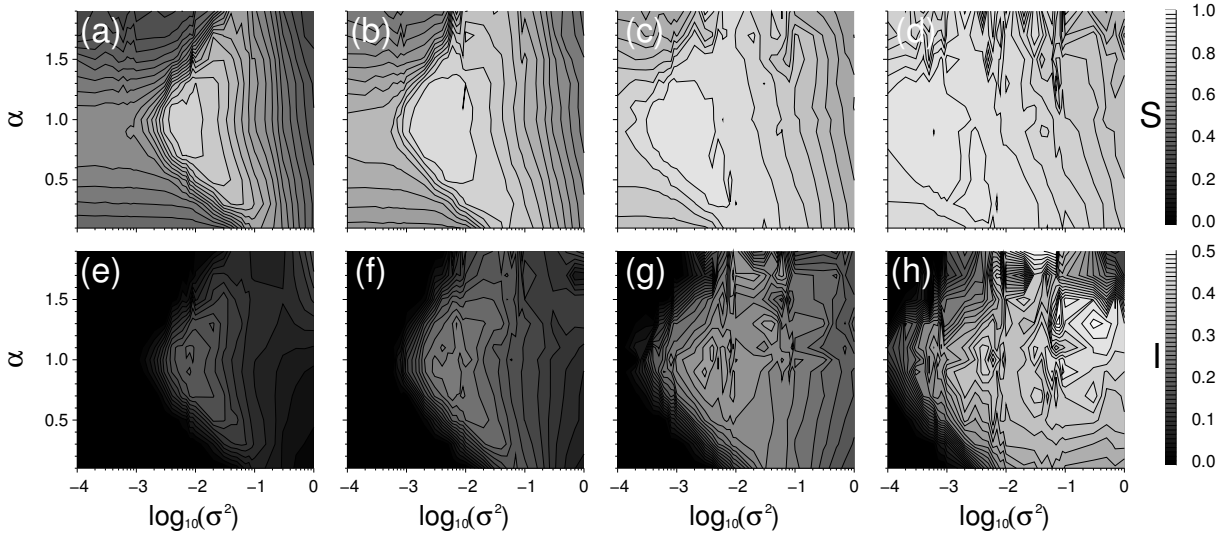

Figure 6.11: Contour plots of the auto-covariance S (a–d) and the mutual information I (e–h) for a sub-excitable network subject to spatiotemporal power-law noise as a function of the noise intensity σ^2 and the temporal noise color. The temporal correlation is denoted by the exponent α of the noise's spectral densities drop-off in temporal Fourier space. The exponent β of the power-law noise's spatial correlation increases from (a,e) $\beta = 0.1$ via (b,f) $\beta = 0.5$, (c,g) $\beta = 1.0$ to (d,h) $\beta = 1.7$. Data points have been obtained by averaging over 8 runs, each time using a different noise realization. The integration time was $T = 65.36t.u.$. $N = 64$, $D_u = 0.2$. For other parameters cf. Fig. 6.10.

noise color β. Quite strikingly, the results from both measures differ substantially for $\beta > 1$, when the influence of the spatial self-affinity of the noise become important. While σ^2_{opt} moves towards smaller noise levels for increasing β, the mutual information shows a slight minimizing effect for σ^2_{opt} around $\beta = 1$.

This result for the auto-covariance S, defined as the quotient of the local spatial amplitude differences I_H and the global spatial variance σ^2_u, can be understood from the relation of the noise-induced local and global order in the system.

The different influence between the power-law and the exponentially correlated noise on spatial synchronization is elucidated in Fig. 6.13. Interestingly, the inhomogeneity I_H as a function of the noise intensity and spatial color assumes a non-monotonous behavior with respect β in the case of power-law noise (Fig. 6.13a), with the position of the maximum moving towards $\beta = 1.0$ for increasing noise intensity. In other words, increasing β in the range $0 \leq \beta < 1$, results in a desynchronization of nearest-neighbors in the medium. This is a effect not present in the case of exponentially correlated noise (Fig. 6.13b). There, I_H shows the same functional dependence on σ^2 and λ as the auto-covariance S (cf. Fig. 6.5 for the qualitatively same result in the case of the mutual information I). Consequently, this hints at the local and global dynamics to be the same everywhere for exponentially correlated noise.

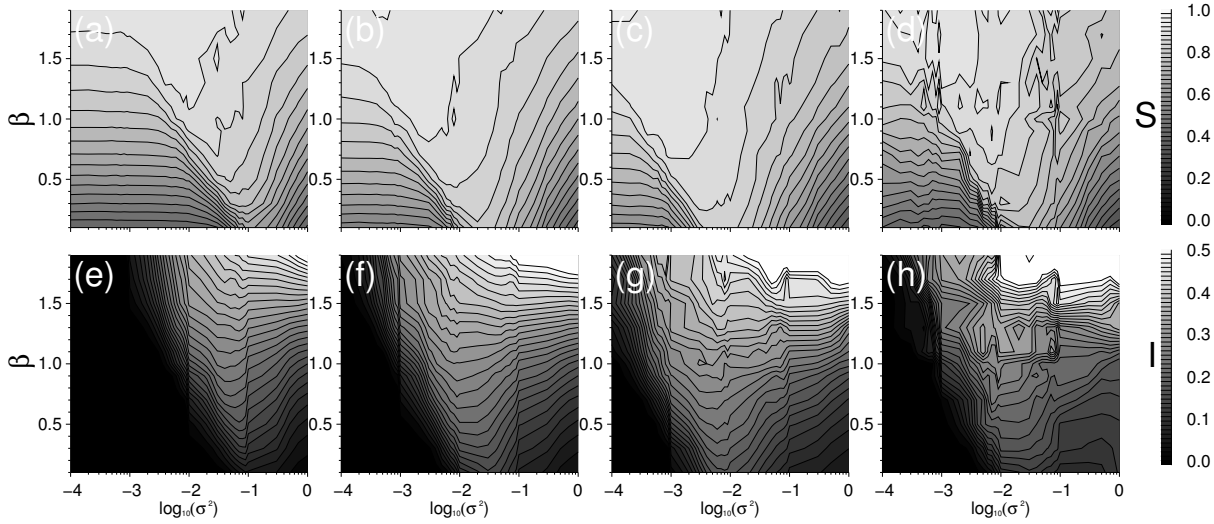

Figure 6.12: Contour plots of the auto-covariance S (a–d) and the mutual information I (e–h) for a sub-excitable network subject to spatiotemporal power-law noise as a function of the noise intensity σ^2 and the spatial noise color. The exponent α of the power-law noise's temporal correlation increases from (a,e) $\alpha = 0.1$ via (b,f) $\alpha = 0.5$, (c,g) $\alpha = 1.0$, (d,h) $\alpha = 1.5$. Data points have been obtained by averaging over 8 runs, each time using a different noise realization. The integration time was $T = 65.36t.u.$. $N = 64$, $D_u = 0.2$. For other parameters cf. Fig. 6.10.

The auto-covariance detects the fingerprint of noise-induced spatial pattern formation from the fact that local excitations induce disproportionately large local amplitude differences, whereas at the same time the global spatial variance σ_u^2 remains relatively unaffected. The self-affine properties of the spatial power-law noise, however, assimilate the local nearest-neighbor (I_H) and the global system variance (σ_u^2). As a consequence, the two measures assume the same values with increasing spatial noise color, the auto-covariance S thus tends to one for large β. This effect therefore superimposes the detection of STSR for long spatial noise correlations, resulting in the monotonous shift of the maxima for S towards smaller values of the noise.

The mutual information I, on the other hand, maps the systems' outputs onto a binary state space, hence effectively filtering out fixed-point fluctuations. This measure therefore detects (correctly) the onset of excitable pattern formation at much higher noise levels. Moreover, one observes an optimization of STSR around $\beta \approx 1.0$ (cf. Fig. 6.12f,g). From an information theoretic interpretation of the system, we therefore conclude that power-law noise optimizes spatiotemporal pattern formation with respect to both temporal and spatial noise color.

The difficulties in simulating power-law noise are quite apparent from the above results. The contour plots show large irregularities despite long and many simulation runs. Especially at high spatial and temporal color, when the noise becomes non-

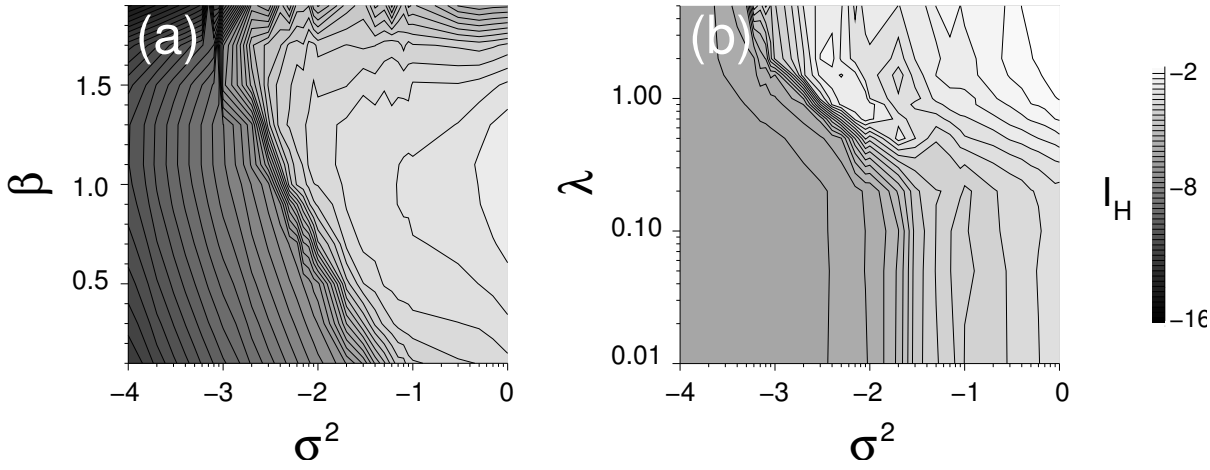

Figure 6.13: The inhomogeneity I_H [Eq. 4.2] of the sub-excitable network as a function of the spatial noise color and the noise intensity. (a) Power-law noise with $\alpha = 1.0$. (b) Exponentially correlated noise with $\tau = 0.1$. $N = 64$, $D_u = 0.2$. For other parameters cf. Figs. 6.10 and 6.3, respectively.

stationary in a strict sense, the errors are discernible. Further numerical simulations would be necessary to improve the statistics. It is an open question, whether values for α,$\beta > 1$ is a useful and valid parameter range with respect to real systems, due to the non-stationarity of the noise. But at least for temporal $1/f^{\alpha}$ noise experimental evidence exists that there are processes showing a power-law behavior with an ever increasing variance in time [Wornell 1993].

Figure 6.14 compares the numerical results for the auto-covariance and the mutual information with the analytical predictions. The relative shift of σ^2_{opt} as a function of α and β yields results similar to the previous section. In the case of S, Fig. 6.14a–c, one observes a monotonous behavior of σ^2_{rel} as a function of β and a maximum around $\alpha = 1.0$ for the temporal noise color. While these results for β are misleading with respect to excitable pattern formation, they unveil the assimilation of local and global dynamics due to the self-similar properties of the noise. The result for the mutual information, on the other hand, now reveals a maximum at intermediate temporal and spatial noise color. The analytical predictions generally agree qualitatively for the dependence on α, but they disagree to a great extend with β (cf. Fig. 6.14f), because the linear response analysis does not take non-local effects like the self-similar behavior of the power-law noise and the resulting multi-scale correlations into account.

Conclusions

Summarizing, we have shown that spatio-temporal noise is beneficial to the occurrence of Spatiotemporal Stochastic Resonance in a sub-excitable medium. The superiority of

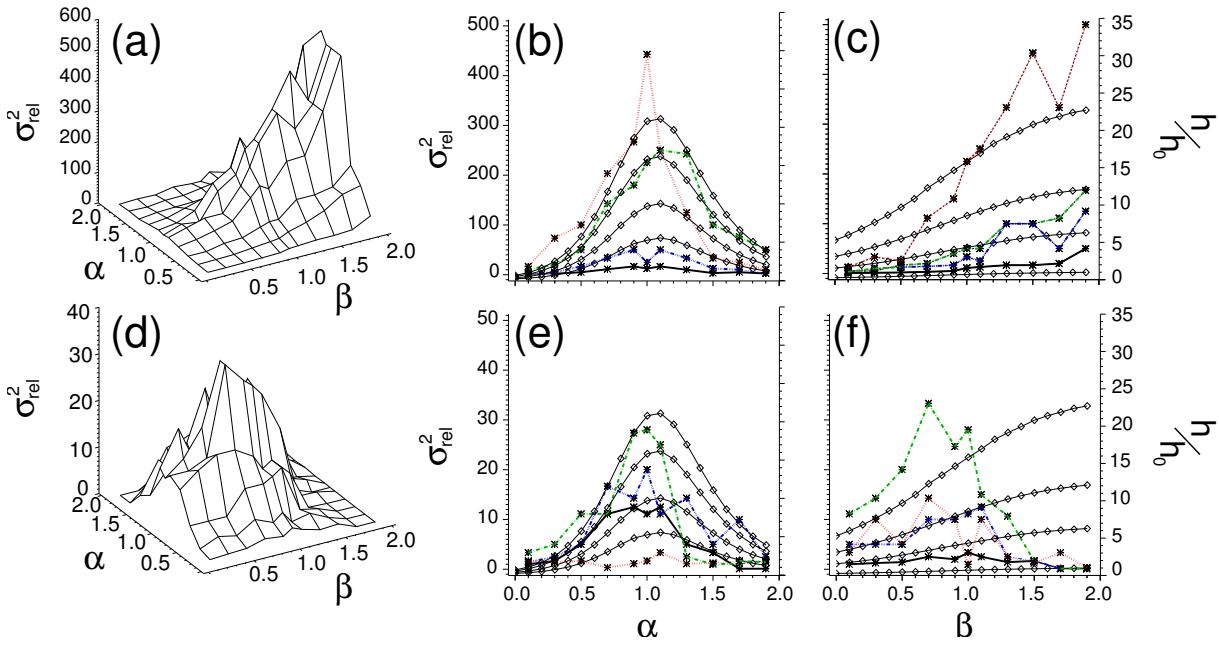

Figure 6.14: The relative shift σ^2_{rel} of the optimal noise intensity for STSR. (a–c) σ^2_{rel} calculated from the auto-covariance S. (d–f) σ^2_{rel} calculated from the mutual information I. (b,e) Cross-sections of the respective surface plots along the α axis. β increases from $\beta = 0.0$ (black, solid line) via $\beta = 0.5$ (blue, $\cdots$–), $\beta = 1.0$ (green, ·–) to $\beta = 1.5$ (red, $\cdots$). (e,f) Cross-sections along the β axis. α increases from $\alpha = 0.0$ (black, solid line) via $\alpha = 0.5$ (blue, $\cdots$–), $\alpha = 1.0$ (green, ·–) to $\alpha = 1.5$ (red, $\cdots$). The solid, diamond marked lines denote the corresponding relative amplification factors $h(\alpha,\beta)/h_0$ [Eq. 3.24].

spatiotemporal colored as compared to spatiotemporal white noise stems from the effective matching between the power spectral densities of the deterministic system and the noise for certain noise color parameters, improving the energy transfer from the noise to the system. The response of the sub-excitable medium with respect to short- and long-ranged correlated noise does not differ substantially for varying temporal noise correlations, but it differs greatly for the spatial noise color. This is explained by the self-affine properties of the $1/k^\beta$ noise and the roughness of the associated noise field. A high spatial correlation therefore does not necessarily postulate synchronization on the local scale. Nearest-neighbor considerations are in turn important for wave nucleation. Hence, there exists an intermediate β for which the relation between the local and global variance is optimal, resulting in a non-monotonous behavior of the pattern forming characteristics with respect to the spatial noise color.

6.2 Spatiotemporal Excitable Dynamics

The excitable state of the network is characterized by the spatially extended system having a second stationary solution, apart from the trivial quiescent state. There exists a non-zero probability that certain initial excitations or inhomogeneous initial conditions lead to stable spiral waves [Tyson & Keener 1988].

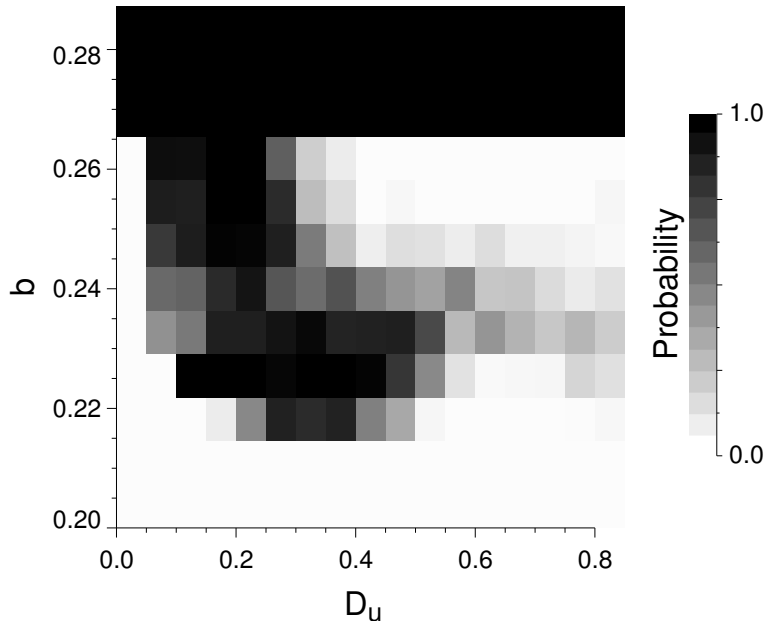

Figure 6.15: Probability for the network to evolve from random initial forcing into the stationary, pattern-forming state as a function of the coupling strength D_u and the bifurcation parameter b. Dark values denote a high probability for the system to sustain moving, self-regenerating waves as a stationary solution. All probabilities have been obtained by averaging over 100 runs, each time using different initial random conditions as well as different noise realizations. The stochastic forcing is switched off after $15t.u.$. Noise parameters: $\sigma^2 = 0.001$, $\tau = 0.01$, $\lambda = 0.01$. System parameters: $N = 64$, $(\epsilon,a,r,\gamma,b) = (0.005,0.5,1.0,1.0,0.24)$.

The border between the sub-excitable and excitable dynamical regimes is controlled by the local excitability of the medium, as discussed in the previous section. Moreover, the probability of random initial conditions to evolve an excitable system into either one of the two solutions depends crucially on the diffusive coupling strength and, once more, the excitability, as can be seen from Fig. 6.15. There, we calculated numerically the probability of the system as a function of the coupling strength D_u and the bifurcation parameter b to evolve into the pattern-forming state after switching off the random forcing of the system. For $b > 0.2683$, beyond the Hopf bifurcation, this probability is one, as all network elements end up in a synchronous oscillatory state, once the transients die out. Within the excitable regime $0.217 < b < 0.2683$, the prob-

ability is maximal for coupling strengths, $D_u < 0.5$, and for low excitability, $b < 0.24$. Both a strong diffusive coupling strength D_u and a high excitability result in a rapid synchronization of the network elements, regardless of the initial conditions, giving rise to global, pulsating patterns that quickly decay to the steady quiescent state of the system. Low coupling and excitability in turn favor the spatially distinct departures of local propagating structures, that can evolve into stable waves and eventually form spiral waves when colliding, leading the system into a pattern forming state.

The role of noise in the excitable regime of the network is thus twofold. Starting the system from its trivial resting state, the stochastic forcing is responsible for nucleating areas of excitation that can stabilize themselves into moving structures. Once stable patterns are formed within the network, the noise disturbs these patterns, i.e. it roughens the wave fronts or breaks up the spiral waves, depending on the noise level. Many investigations deal with the constructive effect of noise on excitable media, such as noise-induced synchronization [Neiman et al. 1999] or noise-sustained pulsating patterns [Hempel et al. 1999]. The onset of new spatial structures out of noise due to the break-up of wave-fronts is a field of active research. [Zhonghuai et al. 1998] showed how parametric stochastic forcing of the Barkley system leads to a noise-induced pattern transition to double armed spirals. The occurrence of noisy spiral turbulence in the same system, whose deterministic dynamics consist of a single, meandering spiral wave, has been studied by [García-Ojalvo & Schimansky-Geier 1999]. The behavior of a spiral wave core in a two-dimensional, complex Ginzburg-Landau equation has been examined by [Aranson et al. 1998], observing Brownian Motion of the spiral tip when driven by white noise.

The rectifying capabilities of an excitable system towards stochastic forcing have also been confirmed experimentally in the BZ reaction. In [Alonso et al. 2001], target waves have been initiated and controlled by a spatially fluctuating illumination field. The noise-induced Brownian motion of a spiral wave has been confirmed in [Alonso & Sagués 2001; Sendiña-Nadal et al. 2000]. There, it was even shown that the effective diffusion coefficient is a non-monotonous function of the temporal noise color.

In the following, we investigate the influence of spatiotemporally correlated noise on the pattern-forming capabilites within excitable systems, setting $b = 0.24$ and the diffusive coupling strength to $D_u = 0.2$. As before, we analyze the effect of short- and long-ranged correlated noise separately.

6.2.1 Spatiotemporal Exponentially Correlated Noise

This section studies the influence of spatiotemporal exponentially correlated noise on moving patterns in an excitable medium. All simulations start from a fully evolved, stable spatiotemporal pattern.
The influence of an increasing noise level is depicted in Fig. 6.16. In the case of weak noise (Fig. 6.16a), the wave fronts remain almost completely smooth and the background, consisting of the network elements fluctuating around their fixed points, remains almost homogenous, as in the noise-free case.

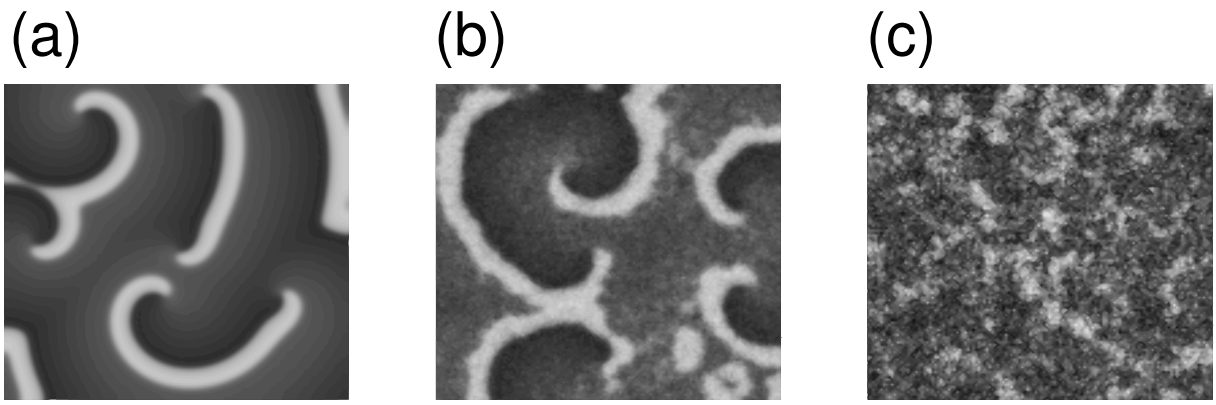

Figure 6.16: Snapshots of the excitable system. The noise intensity increases from left to right (a) $\sigma^2 = 0.001$, (b) $\sigma^2 = 0.01$, (c) $\sigma^2 = 0.1$. All snapshots have been taken after a transient of $10t.u.$. starting from the same initial conditions of stable spatiotemporal, self-regeneration pattern. Noise parameters: $\tau = 0.001$, $\lambda = 0.1$. System parameters: $N = 128$, $D_u = 0.2$, (ϵ,a,r,γ,b) = (0.005,0.5,1.0,1.0,0.24).

The overall behavior of the system becomes more 'turbulent-like' at a moderate noise level. The borders of the structures roughen and new wave nucleation spots are born out of spontaneous excitation or from the fragmentation of wave fronts. These dynamics thus render more complex patterns in the system (Fig. 6.16b). At large additive noise forcing, the size of the patterns decreases dramatically and their coherence becomes lost (Fig. 6.16c).
We can deduce from the above figure that there exists some optimal noise intensity, which is strong enough to let the system explore new regions in phase space, while it is yet weak, such that the lifetime of target and spiral waves is still long enough to transverse the whole system. The excitable medium is therefore in a quasi-turbulent state, which is similar to spiral chaos in deterministic systems [Bär & Eisenwirth 1993].
The cluster-size analysis reflects the above described dynamical behavior. The cluster-size distribution of the almost noise-free case (Fig. 6.17a) has a peak around $n = 600$, accounting for the coherence structures limited in size by the spatial dimensions of the network. Likewise, there is no accumulation of small clusters, contrary to the cluster

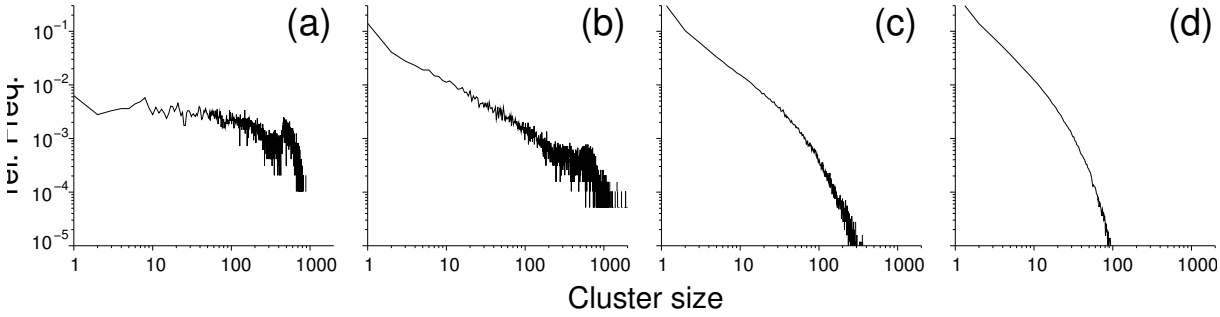

Figure 6.17: Cluster size analysis of the noisy excitable system. The noise strength increases from left to right: (a) $\sigma^2 = 0.0001$, (b) $\sigma^2 = 0.001$, (c) $\sigma^2 = 0.01$ (d) $\sigma^2 = 0.1$. Noise parameters: $\tau = 0.1$, $\lambda = 0.1$. For other parameters cf. Fig. 6.16.

distributions at higher noise intensities in Figs. 6.17b–d. Large noise intensities are clearly marked by a tendency of the distribution towards an increasing size of small clusters in (c–d). At an intermediate noise level, the cluster size distribution obeys a power-law with n with an exponent of $\gamma \approx -1.2 \pm 0.05$, up to the previously discerned peak at $n \approx 600$ in Fig. 6.17b.

It has been argued that noise-induced pattern formation is akin to self-organized criticality (SOC). Previous studies on pattern formation in sub-excitable media, [Wang et al. 1999] and [García-Ojalvo & Schimansky-Geier 1999], identified the power-law exponent of noise-induced structure formation between 2–3 and 1.7, respectively, which is close to the global exponent $\gamma = 2$ [Jung 1997; Paczuski et al. 1996]. Here, however, we find an exponent much lower, which is due to the cluster-size analysis being performed only in space and not additionally in time.

Hence, additive noise in excitable systems induces a higher cluster forming rate, while at the same time these clusters have a high probability to spread and expand up to the spatial scale of the system. This way, one can also speak of noise-enhanced pattern formation in excitable media.

Further statistical analysis using the mutual information I supports these findings in (Fig. 6.18). As expected, we find a functional dependence of I on the temporal and spatial noise color, which is quite similar to the results from the previous section in a sub-excitable network. Nevertheless, there are several differences we want to point out. First, the existence of a maximum for the mutual information at a non-zero noise level supports the visual impression (Fig. 6.16b) of a noise-enhanced pattern formation even in excitable media. The absolute values of these maxima for I are greater than in Fig. 6.4, due to the overall larger cluster size, now spanning the whole network ($I = 0.29$ in Fig. 6.18a as compared to $I_{\max} = 0.17$ in Fig. 6.4a for the sub-excitable system). The position of σ^2_{opt} is generally located at smaller noise levels as compared to

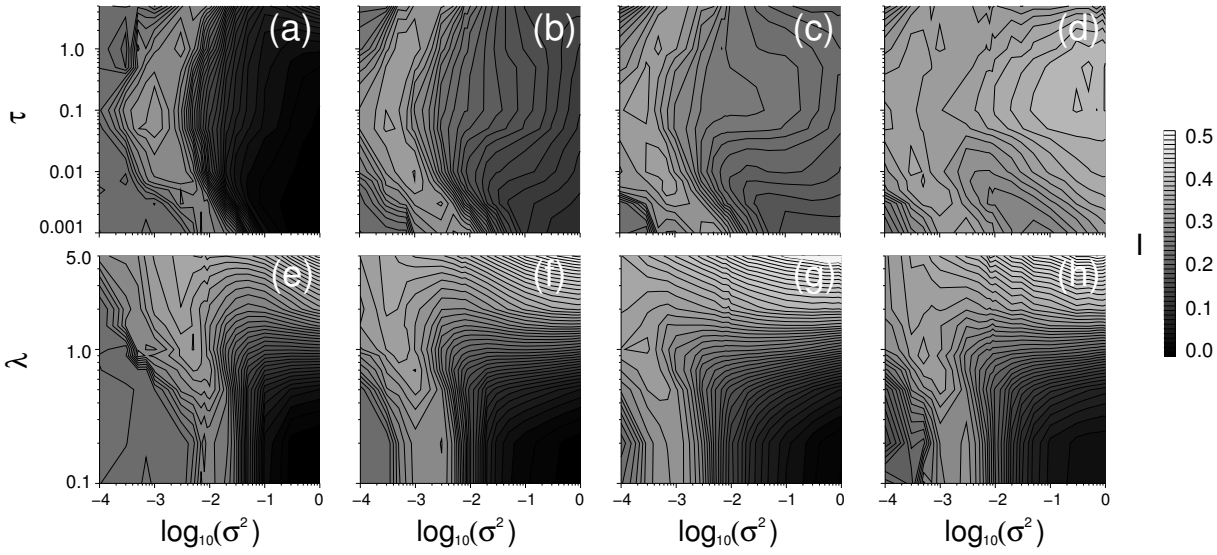

Figure 6.18: Contour plots the mutual information I for an excitable network subject to spatiotemporal exponentially correlated noise. (a–d) I as a function of the noise intensity σ^2 and the temporal noise color τ. The spatial noise correlation increases from (a) $\lambda = 0.1$ via (b) $\lambda = 0.5$, (c) $\lambda = 1.0$, to (d) $\lambda = 5.0$. (e–h) I as a function of the noise intensity σ^2 and the spatial noise color λ. The temporal noise correlation increases from (e) $\tau = 0.001$ via (f) $\tau = 0.01$, (g) $\tau = 0.1$, to (h) $\tau = 1.0$. Data points have been obtained by averaging over 8 runs, each time using a different noise realization. The integration time was $T = 65.36t.u.$. $N = 64$, $D_u = 0.2$. For parameters cf. Fig. 6.16.

the sub-excitable case, owing to the higher excitability of the medium. The transition from purely deterministic excitable pattern formation to the 'turbulent', noise-initiated patterns at small noise intensity is marked by a high, yet constant, level of the mutual information. Large noise intensities and long-range spatial correlations superimpose the first maximum, stemming the noise-initiated pattern formation, with a second one, which is caused by the direct synchronization of the medium due to the spatially correlated noise field. This effect has been previously observed in the sub-excitable medium, yet here, the noise-field synchronization is less pronounced as a consequence of a stronger influence of the excitability on the overall system dynamics (Fig. 6.18d).

6.2.2 Spatiotemporal Power-law Noise

A slightly different scenario is investigated in the context of applying spatiotemporal power-law noise. This time, each simulation run starts from random initial conditions. The contours of the mutual information are akin to the findings in the sub-excitable case, comparing Fig. 6.19 with Figs. 6.11e–h amd 6.12e–h, respetively. Here, I starts from small values for weak noise, increasing not until noise-induced pattern formation becomes possible. The mutual information obtains a boomerang-shaped contour

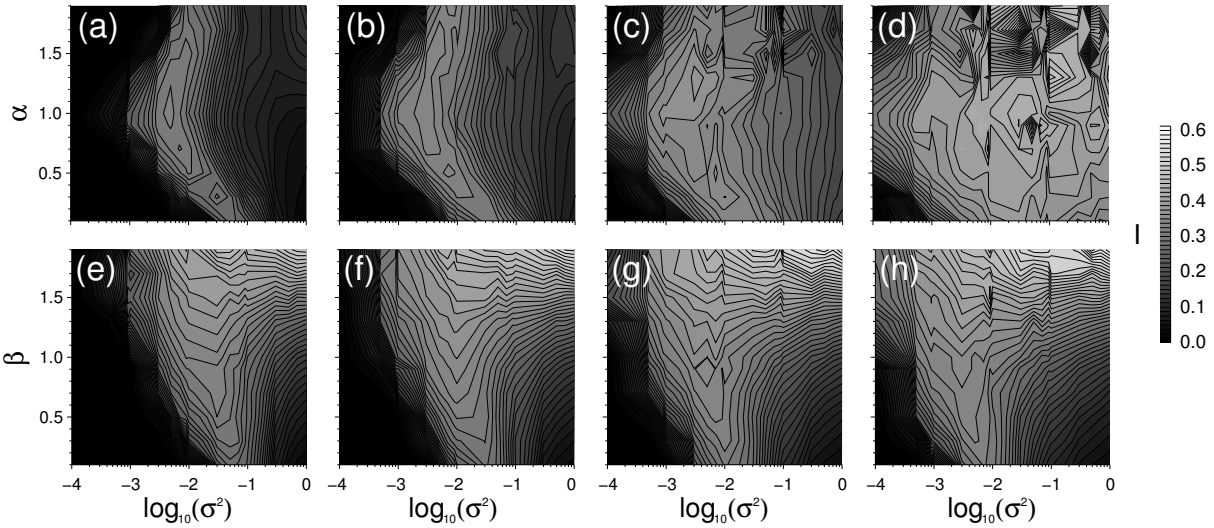

Figure 6.19: Contour plots the mutual information I for an excitable network subject to spatiotemporal power-law noise. (a–d) I as a function of the noise intensity σ^2 and the temporal noise color, denoted by α. The spatial noise correlation increases from (a) $\beta = 0.1$ via (b) $\beta = 0.5$, (c) $\beta = 1.0$, to (d) $\beta = 1.5$. (e–h) I as a function of the noise intensity σ^2 and the spatial noise color β. The temporal noise correlation increases from (e) $\alpha = 0.1$ via (f) $\alpha = 0.5$, (g) $\alpha = 1.0$, to (h) $\alpha = 1.5$. Data points have been obtained by averaging over 8 runs, each time using a different noise realization. The integration time was $T = 65.36t.u.$. $N = 64$, $D_u = 0.2$. For parameters cf. Fig. 6.16.

with respect to α and σ^2 (Fig. 6.19a–d). The influence of excitability is visible from the absolute value of the resonances. Here, we obtain a maximal value of $I_{\max} = 0.31$ in Fig. 6.19a as compared to $I_{\max} = 0.18$ in Fig. 6.11a for the sub-excitable system. The possibility of wave expansion reduces the stochasticity in the system and therefore increases the spatial order, thus leading to overall higher values and sharper resonances for the mutual information. Furthermore, the optimization of Spatiotemporal Stochastic Resonance at an intermediate noise correlation length β is now clearly visible (Fig. 6.19f).

Conclusions

Summarizing, we found that additive, spatiotemporal noise is capable of inducing complex structures in an excitable medium by allowing the system to explore new parameter space regions, while the destructive effect of noise on the coherence of the patterns is not yet pronounced. From an information-theoretic point of view, the medium is thus capable of holding more information.

The findings for the mutual information as a function of the spatial noise color confirms the previous interpretations, which I being maximal for a non-zero noise level. The similarities of the mutual information contours in the sub-excitable and excitable case

reveal the close relationship of these two dynamical regimes.

6.3 Synchronization in an Oscillatory Medium

This section briefly studies the effect of spatiotemporal colored noise on the synchronization of a network of coupled FitzHugh-Nagumo oscillators in the limit cycle regime. As before, one expects the synchronization, or rather the noise-determined desynchronization of the system, to depend strongly on the spatiotemporal noise color as a result of a cooperative process involving the stochastic forcing, the nonlinearity and diffusive coupling.

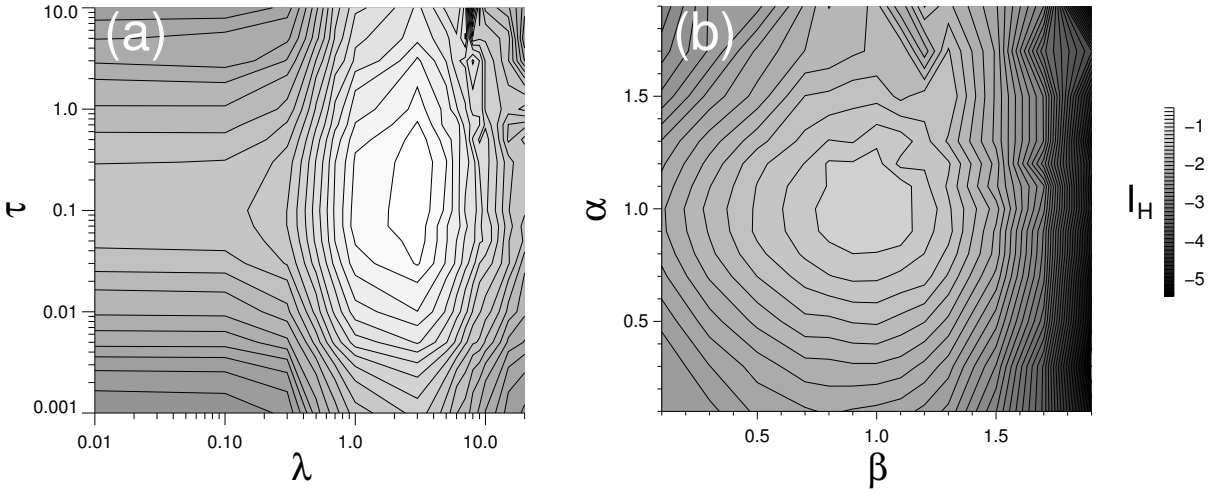

Figure 6.20: The logarithm of the inhomogeneity I_H of the network as a function of the temporal and spatial noise color τ and λ for constant noise variance $\sigma^2 = 0.5$. The integration time was $T = 55t.u.$ with a transient of $T = 5t.u.$. A typical limit cycle oscillation lasts approx. $T = 0.5t.u.$. Four realizations have been performed, each time using a different sequence of the attractor as well as different sets of random numbers for calculating the noise amplitudes. System parameters: $N = 32$, $D_u = 0.2$, $\sigma^2 = 0.1$, $(\epsilon,a,r,\gamma,b) = (0.005,0.5,1.0,1.0,0.5)$. Periodic boundary conditions have been used.

The investigation of synchronization in populations of interacting oscillators is a promising field of ongoing research and is of considerable importance in a variety of physical and biological applications [Kuramoto 1984; Winfree 1980]. Synchronization between oscillators is usually defined in terms of phase differences of variables (cf. [Pikovsky et al. 2001] for a review on the subject of synchronization). Here, we investigate the amplitude synchronization of the network instead, using the inhomogeneity I_H of the fast activator variable u [Eq. (4.2)]. We apply the inhomogeneity for two reasons. First, this measure is directly accessible from the output of the simulations. The definition of a phase at high noise levels oftentimes poses difficulties due to sudden

noise-induced jumps of the oscillator, whereas the inhomogeneity is well defined at all times. Lastly, the activator amplitude of the FitzHugh-Nagumo oscillator is strongly coupled to the phase due to the spiking characteristics of the output. As a consequence, both amplitude and phase synchronization should lead qualitatively to similar results. Considering Eq. (3.7), we set the bifurcation parameter to $b = 0.5$, yielding the local dynamics in the middle of the oscillatory limit cycle regime. In the following, we vary the spatiotemporal correlation lengths τ and λ, the coupling strength D_u and the time-scale parameter ϵ, while most of the time keeping the noise variance fixed at $\sigma^2 = 0.5$.

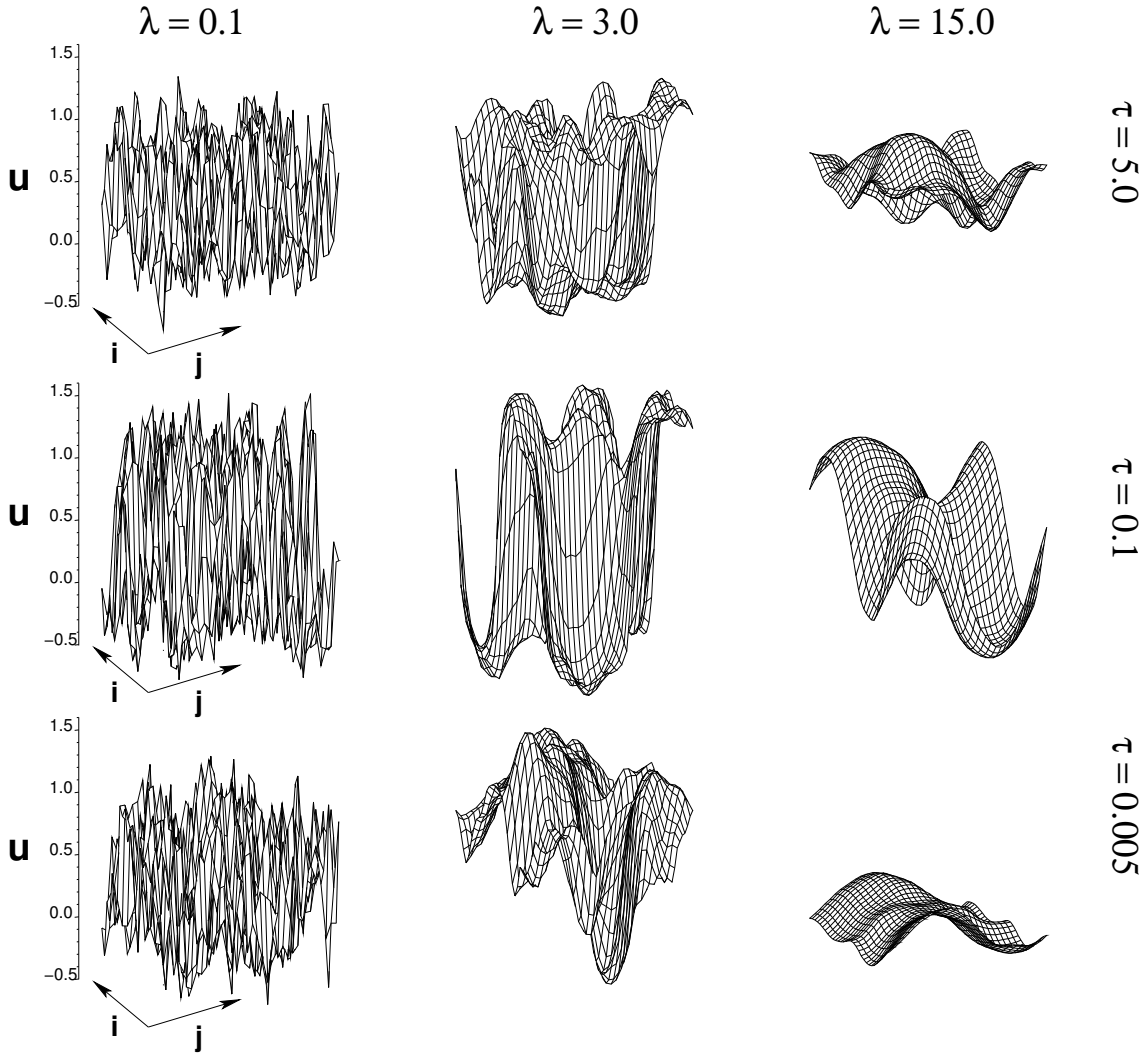

Figure 6.21: Snapshots of the network of coupled FitzHugh-Nagumo oscillators for varying spatiotemporal correlation and constant noise variance $\sigma^2 = 0.1$. τ and λ increase from top to bottom,and left to right, respectively. Snapshots are taken after a transient time of $t = 5t.u.$. For other parameters cf. Fig. 6.20.

The central result is given in Fig. 6.20, which depicts the inhomogeneity as a function

of the temporal and spatial noise correlations, denoted by (τ,λ) and (α,β) for the exponentially correlated and power-law noise, respectively. I_H shows a global maximum, $I_H^{\max}$, at intermediate spatiotemporal noise color for both types of noise, resulting from the combined influence of the temporal and the spatial noise color on the synchronization of the system. While the functional dependence of I_H is symmetric with respect to the temporal noise correlation, this symmetry becomes distorted at large spatial noise color as a consequence of the finite system size.

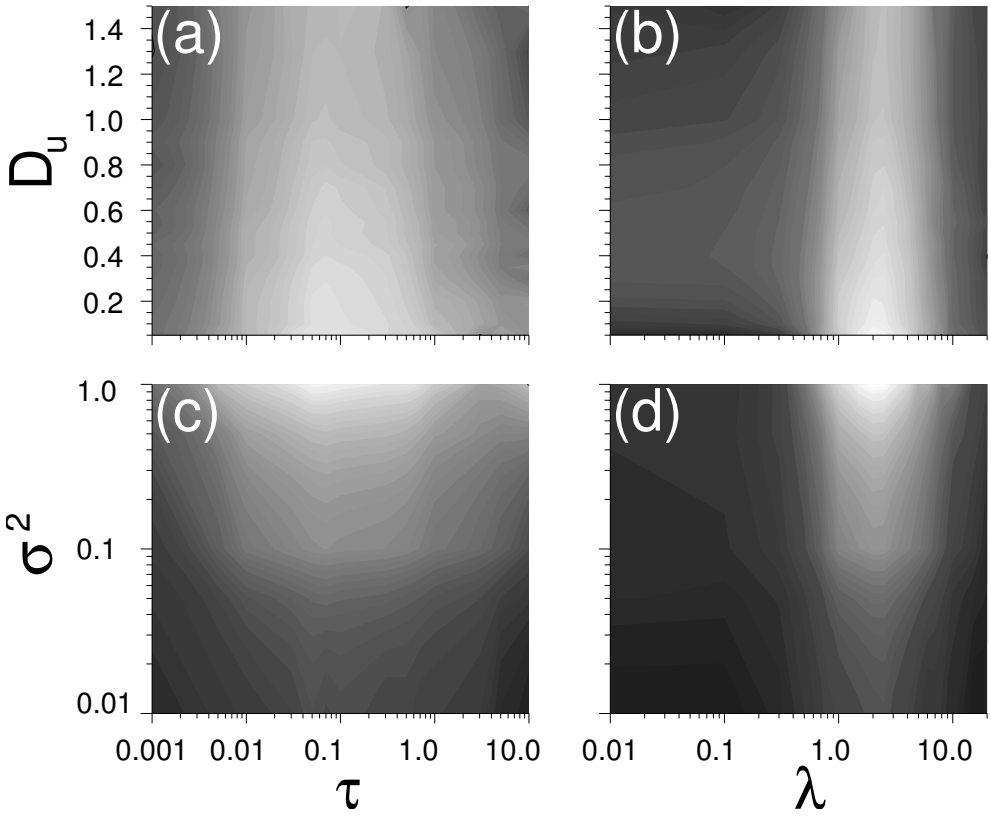

Figure 6.22: The inhomogeneity as a function of the coupling strength (a–b) and the noise intensity (c–d) for varying temporal (a,c) and spatial (b,d) noise color, τ and λ, respectively. The contour plots increase in 30 levels from 0 (black) to 0.4 in the top and to 0.7 in the bottom row (white). The inhomogeneity has been taken at $\lambda = 3.0$ in case of varying τ and at $\tau = 0.1$ at varying λ. For parameters cf. Fig. 6.20.

In Fig. 6.21 some typical snapshots of the system are shown. The effect of varying τ and λ on the desynchronization is clearly seen. The typical oscillator amplitudes show a maximal amplitude $\tau = 0.1$ and $\lambda = 3.0$, which coincides with the maxima from Fig. 6.20a.

The location of the maximal inhomogeneity with respect to the temporal noise color around $\tau = 0.1$ agrees with the result of the investigation on the single oscillator in

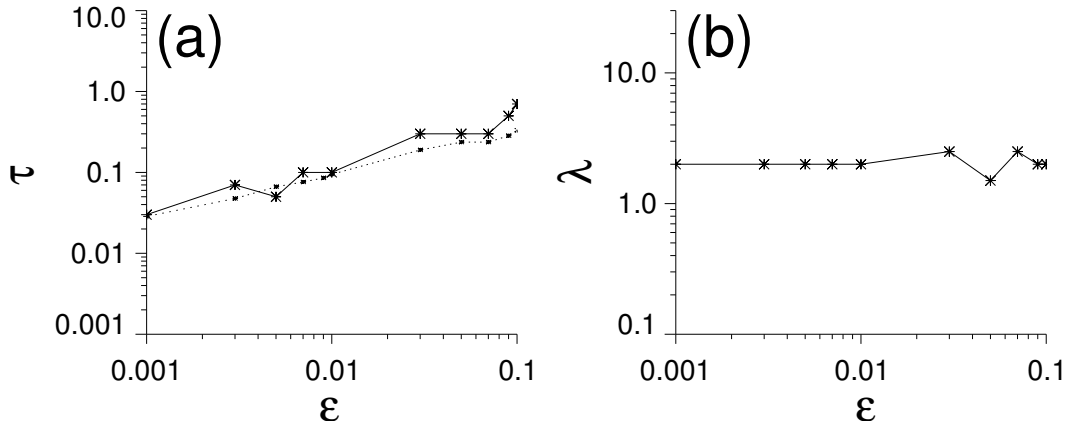

Figure 6.23: The maximal inhomogeneity $I_H^{\max}$ of the network as a function of the temporal and spatial noise color τ and λ for increasing time-scale parameter ϵ. (a) $\lambda = 3.0$. The dotted line denotes the analytical predictions from Eq. (3.24). (b) $\tau = 0.1$. Other parameters cf. 6.20.

Sec. 5.2. A resonance behavior with respect to the spatial noise color has been previously observed in the case of $1/k^\beta$ noise (cf. Fig. 6.19), but now also holds for exponentially correlated noise.

These findings for the FitzHugh-Nagumo system are in good agreement with the previous investigations in [Busch et al. 2001]. There, the average inhomogeneity for a network of biologically motivated limit cycle oscillators as well as a network of coupled, chaotic Lorenz oscillators with changing temporal noise color has been compared, with I_H being maximal at an intermediate noise color.

The location of $I_H^{\max}$ is independent of the coupling strength D_u and the noise intensity σ^2, as can be seen from Fig. 6.22a-b and c-d, respectively. σ^2 neither changes the position nor the shape of the maxima, besides increasing the noise-induced desynchronization. The same applies to the variation of the coupling strengths, which has a smoothing effect on the inhomogeneity, but which does not change the overall functional dependence of I_H on the noise color.

Varying the local dynamics of the medium via the time-scale parameter ϵ, changes the position of the maximal desynchronization with the temporal noise color, $I_H^{\max}$. In analogy to the single oscillator case (cf. Fig. 5.8) and in good agreement with the maxima of the analytical amplification factor $h(\tau)$, the position of $I_H^{\max}$ is shifted towards larger values of τ (Fig. 6.23a). At the same time this parameter shift does not affect the system's behavior with respect to λ.

We therefore conclude, that the location of $I_H^{\max}(\lambda)$ as a function of the spatial noise color is independent of the underlying particular limit cycle system. Indeed, $I_H^{\max}(\lambda)$ is an extensive value, which depends on the system size. Figure 6.24 shows, how the location of this maximum moves in a power-law fashion towards larger values of λ

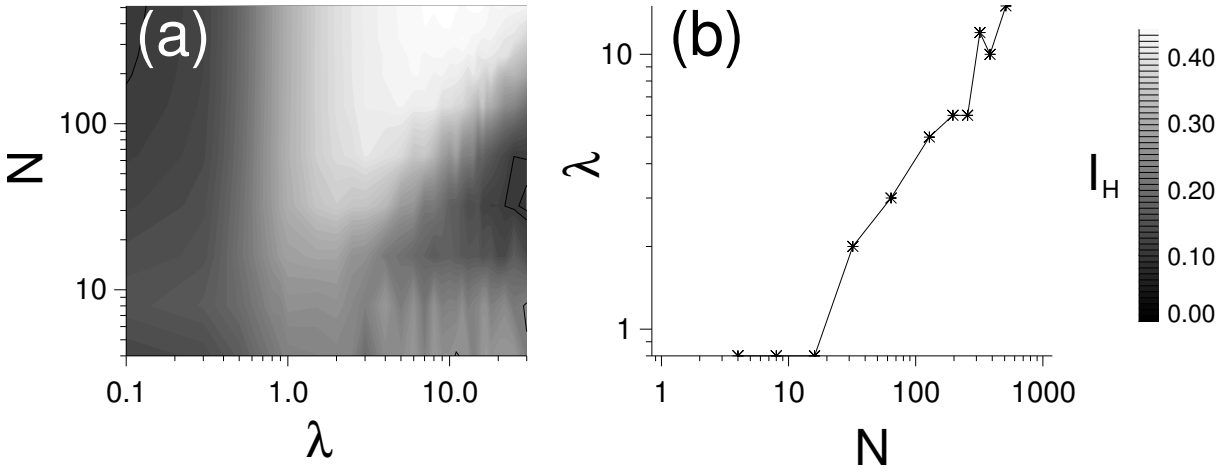

Figure 6.24: The inhomogeneity of the network as a function of the spatial noise color λ for increasing network size, denoted by the side length N for $\tau = 0.1$. Other parameters cf. 6.20.

for increasing network size N. Naturally, one also observes that the notion of spatially correlated noise seems to break down for systems $N < 16$, when it is impossible to clearly define a maximal I_H due to the large errors.
In conclusion, we have seen that varying the spatiotemporal noise color enhances the desynchronization at intermediate spatiotemporal noise color within an oscillatory medium as a consequence of the interplay between the temporal time scales of the single oscillator and the spatial scales on the network level. The resonance of I_H with the spatial noise color is a newly found phenomenon, which is not present in the excitable case. Its exact explanation is yet unclear.

6.4 Discussion

We have analyzed the effect of spatiotemporal colored noise on pattern formation and synchronization in active media. The simulations have shown a strong, yet beneficial influence of moderate spatiotemporal noise correlations on pattern formation or the inhomogeneity in the excitable and oscillatory case, respectively. The quantification of noise-induced pattern formation using the spatial auto-covariance S and the mutual information I generally agree with the visual impression of the pattern forming processes in the excitable media. However, these measures can lead to ambiguous results, especially in the case of spatial power-law noise for $\beta > 1$. The different interpretation of dynamics between the spatial auto-covariance and the mutual information have been explained from the relation of the local and global system states. In the case of spatial power-law, the nearest-neighbor and the overall system variance are of the same order of magnitude, thus S tends to one with increasing spatial noise color. The mutual information, on the other hand, filters small fixed point fluctuations and takes local nearest-neighbor considerations into account, only. It is thus unaffected by the special character of $1/k^\beta$ noise and thus reveals an optimal noise-induced pattern formation for $\beta \approx 1$.
The linear response analysis is in good agreement with regard to the temporal noise color, but shows its limitations in the case of spatial noise color due to finite size effects and in the case of power-law noise, due to its self-affine properties.
One interesting result is how colored noise unveils the hidden dynamical similarities between the various dynamical regimes. Despite the different output dynamics, i.e. oscillatory behavior or excitation pulses, the systems' susceptibility to noise remains the same. This is a consequence of the power transfer from the noise to the system, being mostly dependent on the structure of the null clines, which do not change when switching the medium from its excitable into its oscillatory state.
The table on the next page finally summarizes and compares the main results of this chapter for the different dynamical regimes as well as noise types.

		Exp. Corr. Noise		Power-law Noise
sub-excitable medium	τ	• moderate τ optimizes STSR • $\tau \approx 0.1$ minimizes σ^2_{opt} • detected by auto-covariance S and mutual information I • numerical results in good agreement with analysis	α	• optimal STSR at moderate α • $\alpha \approx 1$ minimizes σ^2_{opt} • detected by auto-covariance S and mutual information I • numerical results in good agreement with analysis
	λ	• λ enhances STSR • monotonous decrease of σ^2_{opt} with λ • network synchronization for large λ and noise intensity σ^2 • simulation and analysis match for small λ, only	β	• β enhances STSR • $\beta \approx 1$ minimizes σ^2_{opt} in the case of analysis using I • monotonous decrease of σ^2_{opt} with β in the case of analysis using S due to self-affine properties of the noise. • simulation and analysis disagree for I: linear response analysis no longer valid for $1/k^\beta$ noise • network synchronization for large β, yet less pronounced
excitable medium	τ	• mutual information I: moderate τ and noise intensity optimize pattern formation • $\tau \approx 0.1$ minimizes σ^2_{opt} • larger spatial patterns result in higher mutual information I	α	• mutual information I: moderate α and noise intensity optimize pattern formation • $\alpha \approx 1$ minimizes σ^2_{opt} • larger spatial patterns result in higher mutual information I
	λ	• monotonous decrease of σ^2_{opt} with λ • less pronounced network synchronization	β	• $\beta \approx 1$ minimizes σ^2_{opt} • no observable network synchronization at large β
oscil-latory medium	τ	• moderate τ maximizes inhomogeneity I_H • location of inhomogeneity maximum $I_H^{\max}(\tau)$ depends on individual oscillator parameters	α	• moderate α maximizes inhomogeneity I_H
	λ	• moderate λ maximizes inhomogeneity I_H • location of inhomogeneity maximum $I_H^{\max}(\lambda)$ depends on system size	β	• moderate β maximizes inhomogeneity I_H

7 Conclusions and Perspectives

The motivation of this thesis was to investigate the influence of spatiotemporal colored noise on pattern formation and synchronization in active media. For this purpose, we developed algorithms for the simulation of noise in higher dimensions, implemented strategies for the efficient numerical integration of partial differential equations in parallel and established analysis tools for the identification of coherent structures from noisy data, comparing the numerical results with a linear response approach for the spatially extended system. The results from the simulations have been found to show new, interesting phenomena arising from the interplay of the spatiotemporal noise, the non-linearity of the medium and the spatial coupling. In conclusion, I have demonstrated that external fluctuations may lead to complex, yet ordered, structures in spatially extended systems. This order is stable under various types of noise, as well as spatiotemporal noise color.

Noise Modeling

The development of integration schemes for stochastic differential equations has gained much interest in recent years [García-Ojalvo & Sancho 1999; Kloeden & Platen 1999], which currently does not leave much room for further improvements. However, the most time-consuming part of numerical integration is the modeling of the noise field itself. Thus, we focused on the improvement of efficient algorithms for the modeling of noise. We compared and identified the most efficient algorithms for the generation of Gaussian distributed random numbers, namely the Mersenne Twister for the generation of uniformly distributed random numbers and the numerical inversion scheme for their transformation into a Gaussian distribution.
There exist two strategies for the generation of temporally correlated noise. The Langevin approach is an indirect method, by which one obtains the desired spatiotemporal auto-correlation function from modeling the movement of a particle in a particular potential. Examples thereof are the Ornstein-Uhlenbeck noise (cf. Sec. 2.2.1), which uses a parabolic potential to produce an output that thus shows an exponential decay in the auto-correlation function. $1/f^{\alpha}$ noise with $\alpha = 1.0$ can be deduced approximately from simulation of a particle in an inverse quadratic potential with a singularity at

zero [Ouyang & Huang 1994]. This method is very fast and efficient, but is restricted to those systems describable by an underlying Langevin equation. The other, generally applicable approach is the Fourier Filtering method. It starts by defining an appropriate filter function which is convolved with a string of normalized, uncorrelated noise. The major drawback of this batch method is its memory burden of the convolution operation.
In general, we distinguish between short- and long-ranged correlated noise. The former correlations are expressible by a finite Fourier transform, i.e. a rational transfer function. For example noise with a memory decaying exponentially or Gaussian-like belongs to this class. Long-range correlated noise is defined via its power spectral density, having a power-law functional shape of the form $1/f^{\alpha}$, resulting in an irrational transfer function. This noise process has an infinite memory and a self-affine structure. The modeling approach departs from defining a fractional differential equation, whose transfer function has the desired properties, from which in turn the filter function is derived. The numerical simulations of power-law noise then clearly showed a fractal structure in the power spectral density.
Efficient modeling of spatially extended noise is in general done by extending the above convolution approach into higher dimensions. Problems arise, if the desired filter kernel is not radially symmetric. We therefore apply the McClellan method, which projects a general, two dimensional filter kernel onto two dimensions by a linear approximation of a higher-dimensional mapping function. We successfully applied this method to generate spatially extended power-law noise in two dimensions and we extend the McClellan transform into three dimensions. The techniques developed for the modeling of higher dimensional noise are generally applicable and can be applied to model noise of any desired property.

The Model

In particular, we investigated the influence of additive, colored noise on the dynamical behavior of the FitzHugh-Nagumo system. A wide class of reaction-diffusion systems have similar non-linearities like the FHN model. From this point of view, the results obtained here are applicable in a rather general way.
An analytical treatment of the numerical results is derived from a linearized version of the full spatiotemporal equations, which catches the essential intrinsic length scales. It is then possible to apply a linear response analysis by interpreting the response of the system to spatiotemporal stochastic forcing as a frequency filtering process from which we derived an amplification profile thus predicting the reaction of the system

towards noise forcing of different spatiotemporal color.
We propose two generally applicable implementations for a parallel numerical implementation scheme using p processors on a $(d + 1)$ dimensional system, both for the noise and the network. The scheme assigns to each processor a $d - 1$ dimensional blocks of network elements to be integrated in time. Synchronization between processes or threads is ensured by the use of blocking calls or mutexes in a distributed or shared memory environment, respectively.

Data Analysis Tools

The identification of coherent patterns from an noisy background requires new approaches for the analysis of the spatiotemporal data. We employed three complementary analysis tools, that are, in their entirety, capable of extracting and quantifying the statistical information of the coherent structures sufficiently. The auto-covariance and the mutual information make use of a nearest-neighbor analysis strategy, in which the global dynamics are deduced from local interactions in a cellular automata-like fashion. The cluster size distribution is a measure of global spatial order in the system. Calculating the distribution's center of mass, one obtains the tendency of the system towards the formation of large or small clusters, respectively. The distribution can be quantified by its center of mass. Amplitude synchronization of oscillatory media has been quantified from the inhomogeneity, which is calculated from the averaged nearest-neighbor distances in the medium. This approach is justified with respect to the particular model equations, whose output amplitude is strongly correlated with the phase.
Testing the tools in the pure noise case, and interpreting the results from the simulations on excitable media, it has been shown that under certain circumstances, one needs to compare the results of all three measures in order to avoid misleading interpretations of the dynamics.

Simulation Results

We investigated the influence of spatiotemporally colored, additive noise on pattern formation in an active medium consisting of diffusively coupled FitzHugh-Nagumo systems in the sub-excitable, excitable and oscillatory regime.
In all cases it has been found that colored noise in both space and/or time is superior to spatiotemporal white noise in terms of optimizing the effect of spatiotemporal stochastic resonance or maximizing the inhomogeneity in the oscillatory case. With the help of the linear response analysis we could show that this effect is due to an ef-

fective matching of the power spectral densities of the spatiotemporal noise and the frequency response of the system. The results from the analytical predictions and the numerical simulations are in good agreement. The validity of the linear model ansatz was confirmed from the comparison of the response of the Barkley system towards temporally correlated noise. The monotonous shift of the STSR with increasing temporal noise color, as predicted from the linear model, was indeed found in the respective simulations on the Barkley system.

In the sub-excitable medium, both short- and long-range correlated noise optimizes STSR at an intermediate correlation time of the temporal noise color. This optimization is seen from both a shift of the noise level for coherent pattern formation towards smaller values, as well as from an increase of the absolute value of the mutual information and the auto-covariance.

We could deduce from the mutual information that new phenomena arise from the use of spatially colored power-law noise. It is capable of optimizing pattern formation at a moderate noise level. This is an effect due to the multi-scale properties of this noise, which cause an interplay of the local dynamics and the global, long-range correlations. Short-range correlated noise, however, displays an monotonous decrease of the noise intensity for optimal pattern formation with the spatial noise color as a consequence of the smoothness of the noise field. This is also the reason for large discrepancies of the results from the numerical simulations and the linear noise model, as the theoretical approach does not take the multi-scale properties of the noise into account.

The effects of the multi-scale properties of the power-law noise on STSR are less apparent in the temporal case, because of the system's wide temporal-frequency response range. However, the sub-excitable medium is a strong low-pass filter with respect to spatial frequencies. Hence, the roughness of the spatial power-law noise field becomes important for power spectra density exponents $\beta > 1$.

The excitable dynamical regime displays a similar response towards spatiotemporal noise. We could show from the cluster size distribution and the mutual information that additive noise of moderate intensity and color optimizes pattern formation with respect to propagating structures in the noise-free system. Fluctuations enable the non-linear medium to exploit new regions in phase space, while leaving the patterned structures intact.

Desynchronization in the oscillatory medium is maximized by both intermediate spatial and temporal noise correlations, regardless of the type of noise. While the increase of the inhomogeneity with respect to the temporal noise can readily be retraced to the noise impact on the single oscillator, the occurrence of the maximum as a consequence of the spatial noise color is due to an interplay of the spatial coupling and the system

size and does not depend on intrinsic single oscillator parameters. Unfortunately, a theoretical explanation of this behavior is still lacking.
It is interesting to note, how the noise is capable of uncovering hidden spatiotemporal length scales. We could show that the response of the oscillatory and excitable systems towards temporally colored noise is rooted in the local dynamics of the individual oscillators. In this way, noise elucidates the relatedness of these different dynamical regimes.

Perspectives

Many open questions remain. In the course of this work, different topics have been explored that should be investigated further. Especially the conceptual understanding of noisy pattern formation and noisy synchronization needs further investigation. To my knowledge, the linear response analysis is the only analytical approach to this kind of problem and has been applied here for the first time to the spatio-temporal case. It would have been desirable in some cases to improve the statistics of the results, but this would have required the access to additional computer power. Further investigations with respect to the system-size for the excitable and sub-excitable media should be performed to fully elucidate the effect of spatially colored $1/k^{\beta}$ noise on the pattern forming behavior.
Yet, in the course of this work, we developed rather general schemes for the numerical techniques of the noise and the non-linear stochastic media and data analysis that could provide the basis for further investigations and which are applicable to many fields of research.
The parallelizing scheme presented in this thesis is easily scaled to three spatial dimensions. So far, there exist only few works on noise-induced or sustained structures in three dimensions [Pérez-Muñuzuri et al. 2000; Zhou & Jung 2000]. Actually, the modeling of (3+1) dimensional systems is an indispensable prerequisite to make quantitative predictions on true natural systems. Structures that might be stable in two spatial dimensions need not be so in three dimensional space and vice versa.
The algorithms for the simulation of spatially extended power-law noise could prove fruitful to fields of research, e.g. in solid state [Dutta 1981] and econo physics [Stanley et al. 2002], where long-range correlated fluctuations are commonly encountered.
The use of the data analysis tools is not restricted to numerical simulations. It has been shown in [Busch & Hütt 2004; Hütt et al. 2002] that these tools should also be capable of handling real-life data, if their resolution is scaled appropriately to apply nearest-neighbor considerations.

One of the open, yet interesting questions is the investigation of the noisy pattern forming process in the context of self-organized criticality. It would be interesting to study the validity of SOC with respect to varying spatiotemporal noise color and short- and long- ranged correlated noise.
The case of quenched noise has not been considered. This is the case, when noise remains static in space and time, i.e. $\tau,\lambda \to \infty$. Some research on this topic exists for the spreading of excitable waves in a 2D medium [Sendiña-Nadal et al. 1998a]. Quenched noise might be important, when discussing the robustness of model equations in biology, where disorder shows up in the variability of parameters, leading to complex pattern formation with respect to spatiotemporal dynamics [Busch et al. 2004].
The use of additive noise is justified in the very general case, if the origin of the noise sources is unknown. In some cases of physical and chemical experiments, when the influence of external noise sources is well known, noise can be implemented as multiplicative noise, leading to such phenomena as Doubly Stochastic Resonance (cf. [Zaikin 2003] for an extensive review). If would be thus worthwhile to study the combined influence of multiplicative and additive noise in a system, both being colored. This way one would not only encounter noise↔system, but also noise↔noise interactions, that should possibly lead to new, rather complex resonance phenomena with respect to spatiotemporal time scales.
Finally, we want to point out the relevance of the result from a biological point of view. As soon as one accepts that a biological system itself may serve as the source of noise, colored noise has to be regarded as a frequent phenomenon in biological system. The constructive role of noise is by now an established fact [Bezrukov & Vodyanoy 1997; Levin & Miller 1996; Russell et al. 1999]. From the results in this thesis, one can conclude that spatiotemporal correlations in the noise lead to new dynamical phenomena, which sometimes cannot be neglected in the modeling of the equations.

A Random Number Generators

The modeling of noise requires the efficient generation of random numbers of some desired distribution function. These numbers are obtained with the help of Random Number Generators (RNG). In general, two classes of RNGs are distinguished: true- and pseudo-random number generators, abbreviated as TRNGs and PRNGs, respectively. The former usually record the output from environmental noise sources and prepare them for the use in experiments, whereas the latter generators refer to mathematical algorithms that are capable of producing number sequences which are indistinguishable from true random numbers by means of statistical analysis. PRNGs are the choice if implementing portable numerical experiments on a computer.
This appendix surveys the possibilities for the generation of true and pseudo random numbers. The efficiency and 'randomness' of PRNGs is compared and strategies for obtaining random numbers possessing different probability density functions are discussed.

A.1 True Random Number Generators

In order to obtain true random numbers, one has to rely on environmental noise sources, whose output is easily accessible in sufficient quantity. Examples of such sources are the successive decay time intervals of some radioactive element or the electronic fluctuations in diodes or transistors. For example the web site www.random.org [Haahr 1998] offers free access to the atmosphere noise recordings picked up from some radio antenna.
More practical access to true random numbers for numerical experiments include the use of computer hardware. Electronic devices are known to show current and temperature fluctuations, having a power-law like spectral density (cf. [Dutta 1981] and references therein). One possibility to make the noise from electronic devices available for numerical simulations is the addition of operation amplifiers to the computer through the use of add-on cards [Davies 2000; Freitag 1999]. Recently, computer chipsets have become available, such as the Intel i810, that support the readout of thermal fluctuations from the computer's CPU [Garzik & Rumpf 2000]. They can be used for generat-

ing sequences of random numbers at a rate of roughly $4 \times 10^8 \text{sec.}^{-1}$

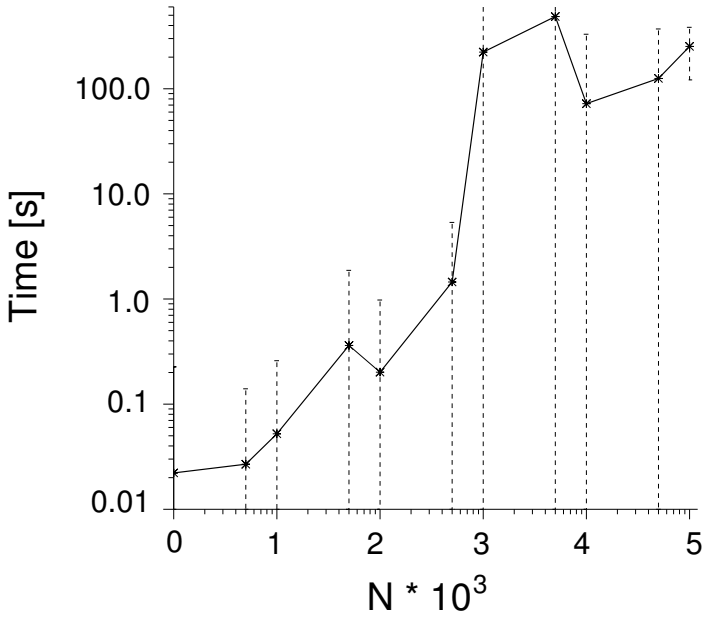

Figure A.1: The average time used to extract N true random numbers from the random device. Note, how the average time depends on the state of the computer. The runs for $N = 1000$ and $N = 5000$ have been performed during nighttime, when the entropy pool fill per unit time is much slower as compared to the day time, which is due to the lack of input from external devices, such as the keyboard or the mouse. The data points have been obtained by averaging over 100 runs each, with the error bars denoting the respective variance.

The Linux operation system offers another possibility to access true random numbers through the special character file `/dev/random`, present in the Linux kernel since version 1.3.30. This device gathers environmental 'noise' from the computer, such as the time intervals between keyboard strokes, interrupt timings, mouse movement and other events, which are non-deterministic. Randomness from these sources is added to an 'entropy pool', from which the random numbers can be extracted [Ts'o 1999]. When read, the device will return random bytes only within the estimated number of bits of noise in the entropy pool. As long as the amount of data extracted from the generator is less than the inherent entropy in the pool, the output data is truly random. For this reason, the routine decreases its internal estimate of how many bits of 'true randomness' are contained in the entropy pool as it outputs random numbers. When the entropy pool is empty, reads to `/dev/random` will block until additional environmental noise is gathered. Quite naturally, due to the sources of randomness, the frequency of input bits is quite low.

Figure A.1 depicts the time for extracting N unsigned long numbers from `/dev/random` as well as the respective extraction variance for extracting the respective amount of

random numbers. The graph clearly shows, that the time increases roughly linearly with the amount of numbers requested from the entropy pool. Tests show that one can extract approximately $30 bytes/sec$ from the random device. Also note how the average time of obtaining N random numbers depends on the time of day. The data points for $N = 10^3$ and $N = 5 * 10^3$ were obtained during night time. Quite naturally, the environmental noise from keystrokes and mouse movements was unavailable during (that particular) night, thus reducing the frequency of input bits.
In conclusion, there exist methods for obtaining true random numbers. Unfortunately, the add-on of readable electronic devices represents a noise generation method that is hardware dependent and that is thus not portable amongst computers. The access to the `/dev/random` device produces random numbers at too low a rate for efficient numerical experimenting. As a consequence, one will have to resort to the use of PRNGs and use the entropy pool as a source for seeding, that is initializing, the pseudorandom number generators.

A.2 Pseudorandom Number Generators

Pseudo-random number generators refer to the implementation of recursive mathematical algorithms that create sequences of numbers $x_i | \, i = 1,2,\ldots n$ which appear random with respect to statistical tests.
In general, there are several criteria that define a 'good' PRNG:

Randomness: a good random number generator produces a sequence of numbers that is indistinguishable from a sequence of independent true random variables. The science or art of tests for randomness touches the foundations of probability and number theory and is beyond the scope of this thesis. Unfortunately, there is no final proof for any PRNG to pass every test of randomness. The more tests it passes, the better. For practical applications, it is rather a question of passing the right tests with respect to the numerical experiment such that it will not spoil or bias the results.

Period: Most random number generators work by iterating some function, mapping the set of integers $\mathcal{N}$ onto itself. Starting from one initial value, the domain will be transversed with (hopefully) no discernable pattern. Obviously, the sequence repeats itself, once a previously visited value occurs again. For this reason, the iterating function and its parameters are chosen to maximize the period to its theoretical maximal length of $\mathcal{N}$. The numerical simulations presented in this thesis,

need approx. 10^{11} random numbers for each run. Practical advice from experience states that no more than 10% of the theoretically available period should be used in order to ensure the randomness of the number sequence. Hence, any PRNG under consideration here needs to have a period of at least 10^{12}.

Memory consumption and speed: Investigating large networks of coupled systems under the influence of noise using long time series, the CPU and memory usage of the PRNG is of some concern. Thus, one has to make some choice between accuracy and speed of the random number generators. For example, nonlinear inverse RNGs offer a great alternative [Hellekalek 1995], if one is not so much interested in speed, but in 'accuracy' of the random numbers, i.e. for the use of Monte-Carlo simulations [Eichenauer-Herrmann et al. 1997; Niederreiter 1995]. Accuracy, meaning the possible failure on some random number test, is not that critical for the noise modeling. Therefore, linear RNGs will be considered, only.

Portability: the code for the model simulations program, including the code for the random number algorithm should be written in a standard programming language so that it can be easily ported onto other computer platforms.

In the following a list of the most commonly used linear PRNGs is presented. For a complete list and extensive study of PRNGs consult the web page of [Hellekalek 2003] at the University of Salzburg.

Linear Congruential Generators (LCG): the simplest PRNGs and still most widely used generators are the so called linear congruential generators, based on the following recursive algorithm:

$$X_n = (aX_{n-1} + b) \; mod \, \mathrm{m}, \tag{A.1}$$

where one has to choose a constant multiplier a, an additive term b, a modulus m and some initial value X_0, called the seed. Equally distributed, floating-point pseudorandom numbers y_n in some interval $[l,u]$ are obtained through the application of the linear mapping $y_n := \frac{u-l}{m} X_n + l$.

The sequence of numbers generated through this algorithm is completely deterministic, i.e. choosing the same seed and parameters will result in the same recursion of numbers. If the constants are chosen appropriately, the output of the algorithm will have a maximal period of m. Usually, the X_i's denote unsigned 32-bit integers and the maximal period of a LCG is hence $m = 2^{32} \approx 10^9$, which

is about 3 orders of magnitude smaller than the required minimal period for the numerical experiments in this thesis.

Famous examples of well-known LCGs are

- the Ansi-C generator with $(m,a,b,x_0) = \left(2^{31}, 1103515245, 12345, 12345\right)$
- the 'Minimal Standard' generator $(m,a,x_0) = \left(2^{31},1,16807, 0\right)$
- the LCG of the NAG group $(m,a,b,x_0) = (2^{59}, 13^{13}, 0, 123456789 * (2^{32} + 1))$
- the Maple random number generator $(m,a,b,X_0) = (10^{12} - 11, 427419669081, 0, 1)$.

Shift-Register generators (SRG): they treat binary numbers of b-bit length as a vector $\mathbf{w}$, also called a word. Once seeded with a non-zero $b-$bit word, a new vector $\mathbf{w_i}$ is formed by a linear transformation. The sequence of random numbers is then generated by the recurrence

$$\mathbf{w}_i = \mathbf{w}_{i-1} \left(\mathbf{I} + \mathbf{R}^r\right) \left(\mathbf{I} + \mathbf{L}^l\right) \forall i > 0, \tag{A.2}$$

where $\mathbf{I}$ is the $b \times b$ unit matrix and $\mathbf{R}$ and $\mathbf{L}$ are the corresponding $b \times b$ matrices performing a right and left bit-shift on $\mathbf{w}$, respectively. Thus, $\mathbf{R}$ contains non-zero elements everywhere except for the principal super-diagonal, $\mathbf{L}$ is zero except for the sub diagonal.

The operation in Eq. (A.2) may be produced by simple computer operations. First form $\mathbf{w}'_{i-1} \leftarrow \mathbf{w}_{i-1} \oplus \mathbf{w}_{i-1}\mathbf{R}^r$, where $\oplus$ denotes a bitwise exclusive-or operation, i.e. a summation modulo 2, next calculate $\mathbf{w}_i \leftarrow \mathbf{w}'_{i-1} \oplus \mathbf{w}'_{i-1}\mathbf{L}^l$. The SRG has a maximal possible period of $2^b - 1$, the number of non-zero realizations of the binary word $\mathbf{w}$. Its advantage lies in the sole use of fast bit-shift operations for the generation of the random number sequences.

Lagged Fibonacci Generators (LF): they are closely related to the SRGs. The Lagged Fibonacci Generators are defined by two lags $p,q > 0 \wedge p > q$ and some arithmetic operation $\diamond$ that may be summation, subtraction, multiplication (all modulo 2) or an *xor*-operation on some $b-$bit word. The algorithm is seeded by an initial set of p-words $\mathbf{w}_i$ in the range of $0 < \mathbf{w}_i < m$. The random number sequence is then generated from the recurrence

$$\mathbf{w}_i = \left(\mathbf{w}_{i-p} \diamond \mathbf{w}_{i-q}\right) \bmod m \quad i \geq p, \tag{A.3}$$

For summation or subtraction the $\mathbf{w}$'s can either be integers modulo 2^k ($k \in \mathbb{N}$) or single- or double precision numbers modulo 1. For multiplication, the $\mathbf{w}$'s have to be odd integers modulo 2^k. A LF generator is easily programmed using a circular list of two pointers. More generalized versions of the LF exist, using 3 or more lag parameters.

Subtract-with-borrow (SWB), Add-with-carry Generators (AWC): this class of random number generators is an extension of the LF algorithm. Additionally to defining two lags p,$q > 0$ and some arithmetic operation $\diamond$, a borrow/carry bit c is introduced. By convention $p > q$. Starting with p initial seeds $\mathbf{w}_0 \ldots \mathbf{w}_{p-1}$ in the range $0 \leq \mathbf{w}_i \leq m$ and an initial value of c, the random number sequence for all $i \geq p$ is generated by calculating

$$t = \mathbf{w}_{i-p} \diamond \mathbf{w}_{i-q} \diamond c \tag{A.4}$$

and setting the new seed and borrow/carry bit as follows

$$\mathbf{w}_i = \begin{cases} t \bmod \mathrm{m} & : \quad 0 \leq t \\ t + m & : \quad \text{otherwise} \end{cases} \tag{A.5}$$

$$c = \begin{cases} 0 & : \quad 0 \leq t \\ 1 & : \quad \text{otherwise} \end{cases} \tag{A.6}$$

The SWB/AWC generators have been first proposed by [Marsaglia & Zaman 1991]. They can reach much longer periods than the underlying LF generators, e.g. up to 10^{171} for the parameters (p,q,m) = (24,10,2^{24}).

A.2.1 Random Number Generator Tests

The quality assurance of random number generators has drawn much attention since the thriving of computers, because poor generators will lead to biased results in simulations. Especially Monte Carlo simulations are sensitive to hidden errors or bias of the PRNGs [Ferrenberg et al. 1992].
A few remarks on the term 'random' are in order. Randomness refers to the process of generating a sequence of numbers $\{n\}$ that exhibits properties reflecting the generating process, where the stress is put on the term 'generating'. It is thus *not* the overall probability distribution $p(n)$ that is characteristic for $\{n\}$, e.g. some sorted, and hence non-random list, could easily have the same statistical properties as $\{n\}$. Instead, one has to use the concept of unpredictability: from the knowledge of some number n_i one should not be able to predict the value of n_{i+1}. In other words, any conditional

probability of n_i is equal to its unconditional one

$$p(n_i|n_1,\ldots,n_{i-1}) = p(n_i). \tag{A.7}$$

Furthermore, it is reasonable to assume that all unconditional probabilities $p(n_i)$ are equal. Consequently, a number sequence $\{n\}$ can be defined as random, if all its joint probabilities factorize

$$p(n_1,\ldots,n_i) = \prod_{k=1}^{i} p(n_k), \tag{A.8}$$

This criterion for randomness can be measured with the use of cumulants. Defining an i-dimensional generating function $G_{n_1\ldots n_i}(s_1\ldots s_n)$ (cf. Sec. 2.1) on the usually unknown probability density $p(n_1,\ldots,n_i)$ and taking into account Eq. (A.8), one finds [Schulten & Kosztin 2000]

$$G_{n_1\ldots n_i}(s_1\ldots s_n) = \prod_{k=1}^{m} \int dn_k p(n_k) e^{is_k n_k} = 1, \tag{A.9}$$

Taking the logarithm of Eq. (A.9) and Taylor-expanding the results, leads to the following expression

$$\ln\left[G_{n_1\ldots n_i}(s_1\ldots s_n)\right] = \sum_{m_1\ldots,m_i=0}^{\infty} \ll n_1^{m_1}\ldots n_i^{m_i} \gg \frac{(is_1)^{m_1}}{m_1!}\ldots\frac{(is_i)^{m_i}}{m_i!}. \tag{A.10}$$

Hence, one can verify the randomness of a number sequence by checking whether the cumulants $\ll n_1^{m_1}\ldots n_i^{m_i} \gg$ of all orders $1 < (m_1\ldots m_i)$ are all zero. Practically, this condition is computed by expressing the cumulants through the moments of $\{n_i\}$ [Risken 1984], which in turn are easily calculated by taking the respective arithmetic averages of the random number sequences $n_1\ldots n_i$.

The various ensembles of random numbers needed for the calculation of the cumulants can be taken from a single random number sequence. Any PRNG on a computer operates on a finite number domain. It thus has a finite period. Consequently, restarting a random number sequence with j different seeds is equivalent to applying a cyclic shift operation on the number sequence

$$S_k(n_i) = n_{(i+k)\mathrm{mod}m}, \tag{A.11}$$

where k is the number of indices shifted and m denotes the period of the algorithm.

The method detailed above is the essence of all random number generator tests. They differ in their particular application of Eq. (A.10). Others tests for randomness determine the number distribution in higher dimensional space (spectral tests) [Knuth

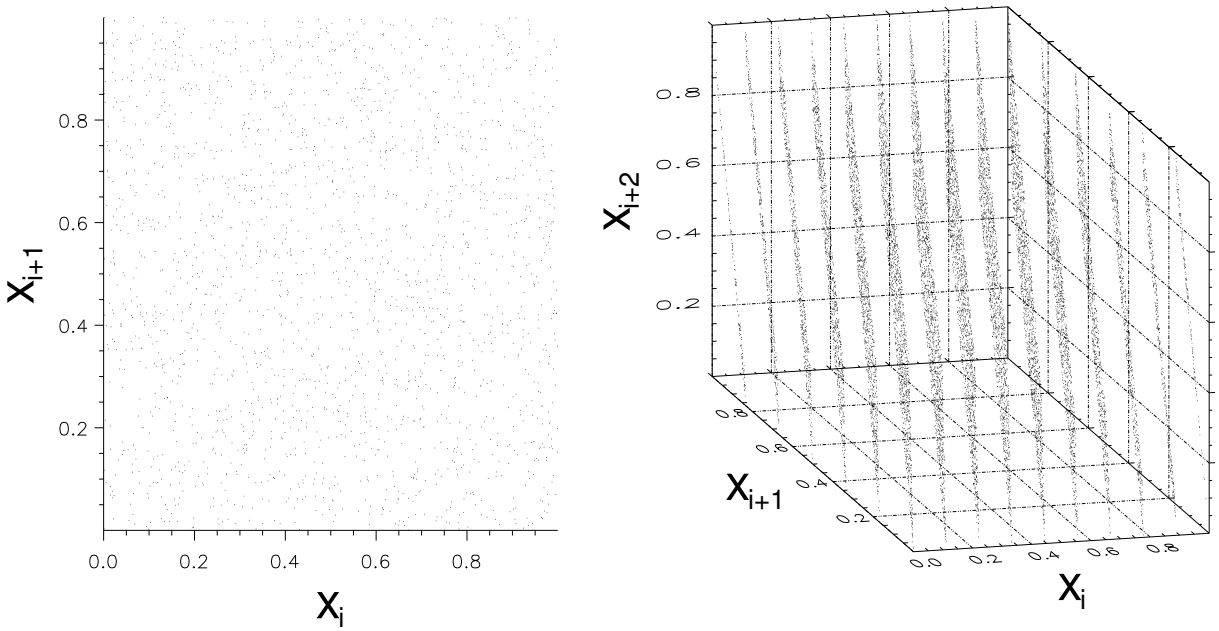

Figure A.2: Scatter plots of adjacent number doublets and triplets of a pseudorandom number sequence generated using a linear congruential algorithm (Eq. (A.1)) with $m = 2^{31}$, $a = 65539$, $b = 0$ and a starting seed $X_0 = 1$. Random numbers are equally distributed in two dimensions whereas 3-tuples show a highly regular distribution, being distributed in 15 planes, only.

1981], search for the occurrence of certain numbers patterns (monkey tests) [Marsaglia 1993] or calculate the entropy of the output number sequence [L'Ecuyer et al. 1996]. For an exhausting review on such tests confer to [Knuth 1981]. There are also program packages for testing random number sequences freely available online. The most popular of these is the DIEHARD program library by [Marsaglia 2003].

Unfortunately, testing for cumulant correlations is very tedious and is, in most cases, restricted to low order cumulant correlations, only. Moreover, to make things even more complicated, there is no final proof that a PRNG produces random number sequences that mimic true random numbers under any circumstance. Even if the algorithm has passed all known test, there could still be some other statistical test invented that the PRNG is vulnerable to. One notorious example where correlations appear in higher-order dimensions is illustrated in Fig. A.2. A scatter plot of number doublets (plotting $x_i$vs.x_{i+1}) seems pretty much random, whereas the same correlation analysis for triplets reveals that the random numbers fall into 15 planes, only. The numbers in these triplets are not completely independent of each other, and consequently they are not 'truly' random. The failure of the PRNG on some statistical test may or may not have an impact on the numerical experiment under investigation. The linear congruential generator with these specific parameters, for example, works fine in the case

of sampling a two dimensional phase space, but is insufficient if sampling a three-dimensional density function.

A.2.2 The Mersenne Twister

The pseudorandom numbers for noise modeling in this dissertation have all been generated by the use of yet another linear random number generator, called the Mersenne Twister (MT). This PRNG has been developed by Matsumoto et al. in a series of papers [Matsumoto & Kurita 1992, 1994; Matsumoto & Nishimura 1998]. The MT is based on a Generalized Feedback Shift Register Generator(GFSR), first proposed by [Lewis & Payne 1973].
The Mersenne Twister outputs a sequence of word vectors $\mathbf{w}_i$, uniformly distributed between 0 and 2^b-1 and having a maximal period of $m = 2^{19937}-1$, which is a Mersenne prime (hence the name), at low computational cost, passing many tests on randomness. The algorithm is based on the following linear recurrence

$$\mathbf{w}_{i+n} := \mathbf{w}_{i+m} \oplus \left(\mathbf{w}_i^u | \mathbf{w}_{i+1}^l\right) A, \quad (k = 0,1,\dots), \tag{A.12}$$

where n is the working area, A a constant binary $b \times b$ matrix, and $\left(\mathbf{w}_k^u | \mathbf{w}_{k+1}^l\right)$ denotes a concatenation of the most significant $u = b - r$ bits of $\mathbf{w}_k$ with the lower $l = r$ bits of $\mathbf{w}_{k+1}$.
To start, the algorithm is initialized with n random seeds. One iterative step is performed by first concatenation, then multiplication of the matrix A of the form

$$A = \begin{pmatrix} & 1 & & & \\ & & 1 & & \\ & & & \ddots & \\ & & & & 1 \\ a_{w-1} & a_{w-2} & \dots & \dots & a_0 \end{pmatrix} \tag{A.13}$$

from the right, tempering the higher and lower bits of $\mathbf{w}_i$ with an appropriate, invertible $b \times b$ matrix before finally adding (modulo 2) $\mathbf{w}_{i+m}$ to this vector. If $r = 0$ and $A = I$, the identity matrix, then this algorithm reduces to the GFSR. The 'twisting' by the matrix A before the addition operation, the tempering and concatenation are performed to obtain a maximal spectral distribution of random numbers. For details cf. [Matsumoto & Nishimura 1998]. The current parameters used for the MT are the following: (b,n,m,r) = (32,624,397,31).
Table A.1 displays the results from tests run on some PRNGs introduced in this section. One can clearly see that the Mersenne Twister in the improved version [Wagner 2003]

	LCG	SR	AWC	MT (orig.)	MT (improv.)
Period	2^{32}	$2^{32}-1$	10^{171}	$2^{19337}-1$	$2^{19337}-1$
Time/Run [s]	8.765	15.456	11.222	4.21	1.920

Table A.1: The table shows the average time for various random number generators to produce a sequences $3 * 10^9$ numbers. The LCG is tested using the standard ANSI-C rand.c function. The SRG algorithm is taken from the Boost C++ library [C++Boost 2003]. The AWC algorithm is implemented using the C program provided by its inventor [Marsaglia & Zaman 1991]. The Mersenne Twister is tested using the original C implementation, available from the MT homepage [Matsumoto 2003]. The improved version has been developed by R. Wagner [Wagner 2003]. All tests have been performed on an AMD Athlon XP 2800 CPU, 1GB RAM, using a 2.4.20 Linux kernel. The algorithms have been compiled with the GNU gcc compiler under the optimization flag '$-O3$'.

is by far the fastest of all algorithms and shall be henceforth used in all simulations.

A.3 Continuous Distributions

One may ask why it is important to be able to generate uniform random variables, since observed distributions are rarely of that form. The reason is that in principle any random phenomenon can be simulated by taking a suitable transformation of a sequence of uniform random variables [Honerkamp 1990].
From the fact that for a coordinate transform $x \to y(x)$ and the inverse transform $x = x(y)$ one has:

$$1 = \int_I \mathrm{d}x\, p(x) = \int_{I'} \mathrm{d}y \left|\frac{\mathrm{d}x}{\mathrm{d}y}\right| p(x(y)) = \int_{I'} \mathrm{d}y\, \tilde{p}(y) \tag{A.14}$$

it thus follows that

$$\tilde{p}(y) = p(x(y)) \left|\frac{dx}{dy}\right| \tag{A.15}$$

is the transformed probability density of the coordinate transform $x \to y(x)$.
Setting $p(x) = 1$ in the interval [0,1], one has to solve for

$$\frac{\mathrm{d}x}{\mathrm{d}y} = \tilde{p}(y), \tag{A.16}$$

and hence

$$x(y) = \tilde{P}(y) = \int^{y} \tilde{p}(y')\, dy'. \tag{A.17}$$

It thus follows for the desired stochastic variable y, having the desired probability density $\tilde{p}(y)$

$$y = \tilde{P}^{-1}(x). \tag{A.18}$$

Take for example the Lorentz distribution. From

$$\tilde{p} = \frac{1}{\pi}\frac{1}{1+y^2}\ , \tag{A.19}$$

it follows that

$$x(y) = \frac{1}{\pi}\arctan(y) \tag{A.20}$$

and for its inverse one has

$$y = \tan(\pi x) \qquad x \in [0,1]. \tag{A.21}$$

Transforming uniformly distributed random numbers according to Eq. (A.21) results in some Lorentz probability density.

The above described method can be expanded into N-dimensions. Let $(X_1,X_2,X_3,\ldots,X_n)$ be a n-tuple of random variables and $\mathbf{x} \leftarrow \mathbf{y}$ the transformation $y_i = y_i(\mathbf{x})$, it then follows for the probability density of the random vector $\mathbf{y}$

$$p(\mathbf{y}) = \left|\frac{\partial(x_1,\ldots,x_n)}{\partial(y_1,\ldots,y_n)}\right| p(\mathbf{x}). \tag{A.22}$$

For example, let (x_1,x_2) be random numbers, uniformly distributed in [0,1]. Transforming them according to

$$\begin{aligned} y_1 &= \sqrt{-2\ln x_1}\cos(2\pi x_2) \\ y_2 &= \sqrt{-2\ln x_1}\sin(2\pi x_2), \end{aligned} \tag{A.23}$$

it follows for

$$\left|\frac{\partial(x_1,x_2)}{\partial(y_1,y_2)}\right| = \frac{1}{\sqrt{2\pi}}\exp\left(-\frac{1}{2}y_1^2\right)\frac{1}{\sqrt{2\pi}}\exp\left(-\frac{1}{2}y_2^2\right). \tag{A.24}$$

Hence, the above two dimensional transform converts two uniformly distributed random numbers into two normally distributed ones. This transform is called the Box-Müller algorithm. Albeit this algorithm being exact, it has the main drawback of being slow. For each random number one has to calculate a sine, cosine, logarithm and a root, all being functions that are expensive with respect to CPU usage. For greater efficiency, it is possible to transform the algorithm to polar coordinates [Press et al. 1993].

Using the identity

$$\begin{aligned} \sin(x_2) &= \frac{x_1}{r} \\ \cos(x_2) &= \frac{x_2}{r} \\ r &= \sqrt{x_1^2 + x_2^2}, \end{aligned} \tag{A.25}$$

where x_1,x_2 are uniformly distributed numbers in the interval $[-1,1]$, one obtains two normally distributed numbers by calculating

$$\begin{aligned} y_1 &= \sqrt{-2\ln(r^2)}\,\frac{x_1}{r} \\ y_2 &= \sqrt{-2\ln(r^2)}\,\frac{x_2}{r}. \end{aligned} \tag{A.26}$$

The extra cost for discarding random numbers for which $r^2 > 1$ is by far outweighed by the benefit for not having to calculate the trigonometric functions.

Numerical Inversion Method

Not every probability density has a distribution function that is readily expressible in terms of elementary functions. This particular problem arises in the case of the Gaussian function, because its inverse function $\tilde{P}^{-1}(x)$ is related to the inverse error function

$$\tilde{p}(y) = \frac{1}{\sqrt{2\pi}}\, e^{\frac{y^2}{2}} \tag{A.27}$$

$$\tilde{P}(y) = \int_{-\infty}^{y} \tilde{p}(y')\,\mathrm{d}y' = \frac{1}{2}(1 + erf[y/\sqrt{2}]), \tag{A.28}$$

where erf denotes the error function, whose inverse cannot be expressed analytically.

One alternative is to perform the transformation of the Gaussian probability density in higher dimensions, resulting in the Box-Müller algorithm. But as noted previously, this is procedure is slow and inefficient.

Instead, the numerical inversion method calculates the inverse function numerically [Hörmann & Leybold 2003] or uses, in this case, a piecewise linear, tabulated approximation of $\tilde{P}^{-1}(x)$ [Toral & Chankrabarti 1993], whose values are stored in an array to be reused anytime a random number is requested. $\tilde{P}^{-1}(x)$ is approximated by the follow-

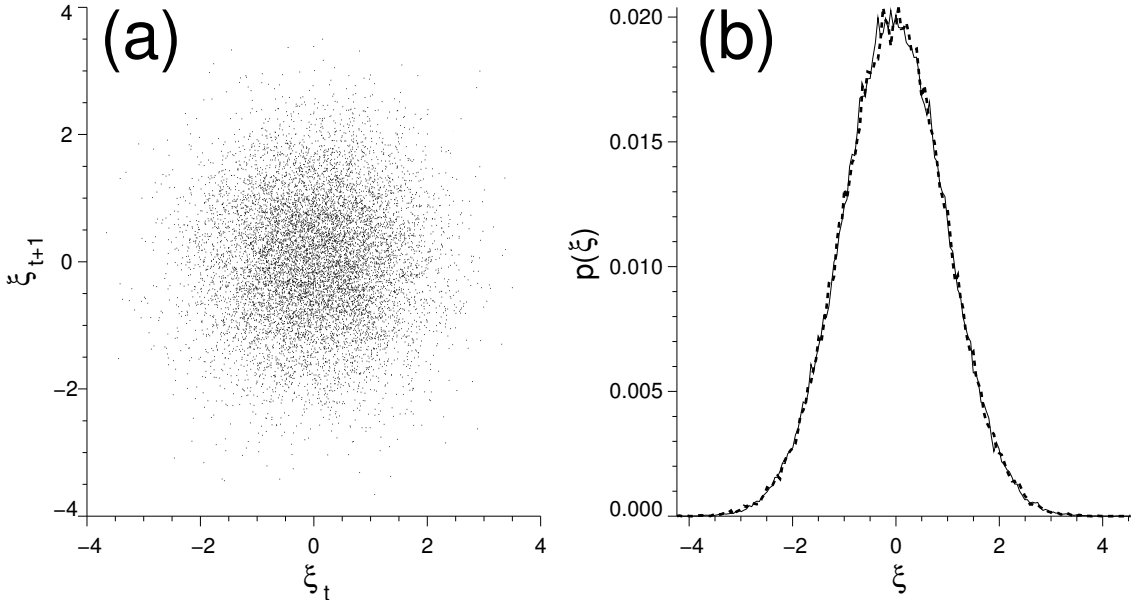

Figure A.3: (a) Normal distributed random numbers using the numerical inversion technique. (b) The probability density of the random numbers obtained by the Box-Müller algorithm (solid line) and the inversion method (dotted line). Parameters: bin size = 0.05, $\sigma^2 = 1.0 < \xi >= 0.0$.

ing rational function

$$\begin{aligned} y &= s - \frac{c_0 + c_1 s + c_2 s^2}{1 + d_1 s + d_2 s^2 + d_3 s^3} + \epsilon \\ s &= \sqrt{-2\log(1-x)}. \end{aligned} \tag{A.29}$$

With the parameters

$$\begin{aligned} (c_0,c_1,c_2) &= (2.515517,0.802853,0.010328) \quad \text{and} \\ (d1,d_2,d_3) &= (1.432788,0.189269,0.001308), \end{aligned}$$

the truncation error of the above approximation is $\epsilon < 4.5 \times 10^{-4}$.

The table inversion method divides the range of x, a uniformly distributed number in [0,1], into m subintervals, storing their function values $y_i = \tilde{P}^{-1}(i/m) | \, i = 0, \ldots m$. The Gaussian distributed random numbers y are then calculated by slotting each uniformly distributed random number $x | 0 < x < 1$ into its respective interval $i = \text{int}[m * x]$ and interpolating linearly between y_i and y_{i+1} according to

$$y = (mx - i)y_{i+1} + (i + 1 - mx)y_i, \tag{A.30}$$

where int$[m * x]$ denotes the integer part of $m * x$.

	Rand. Int.	Box-Müller	polar Box-Müller	Num. Inversion
Rel. Speed	1	24.36	19.20	1.09

Table A.2: The relative CPU time for generating normally distributed random numbers. The run times were evaluated in quadruple, generating 5×10^8 random numbers in each run. The random numbers have been generated using the Mersenne Twister RNG (Sec. A.2.2). The relative speed does not include the calculation of the lookup table for the inversion function $\tilde{P}^{-1}$ in the case of the numerical inversion technique. Using an array of length of only 2^{14} its creation time is almost negligible. All test have been performed on an AMD Athlon XP 2800 CPU, 1GB RAM, using a 2.4.20 Linux kernel. The algorithms have been compiled with the GNU gcc compiler under the optimization flag '$-O3$'.

Reasonable parameters for the number of intervals, and hence the resulting cut-off values of the Gaussian distributed random numbers y are $m = 2^q = 2^{14}$ and $|y|_{max} = 3.842$, respectively [Toral & Chankrabarti 1993]. The efficiency of the table inversion method derives from the fact that the calculation of the y's [Eq. (A.30)] only require additions and multiplications. Furthermore, noting that uniformly distributed numbers in the interval [0,1] usually are calculated by the ratio of $UL/2^n$, where UL is a random bit sequence of length $b = 32$, the appropriate slot i can be calculated efficiently by the bit-shift operation $i = UL * 2^{q-b}$, if choosing $m = 2^q$.

If suitably normalized, the inversion method returns approximate Gaussian distributed numbers between $-3.842 < y < 3.842$, having a mean value of zero and a standard variance $\sigma^2 = 1$. Other distributions having a different mean m' and variance σ'^2 can be generated by the linear transformation $y' = \sigma' y + m'$. The output from the table inversion method is depicted in Fig. A.3. Both the scatter plot (a) and the probability density function (dotted line in b) clearly exhibit Gaussian functional properties, being in almost perfect agreement with random numbers generated via the polar Box-Müller algorithm [Eq. (A.26)]

Table A.2 shows the relative CPU usage to generate normally distributed numbers. The numerical inversion method is about 10 times faster than the standard Box-Müller algorithm, and it is hardly slower than the direct generation of integer random numbers. In conclusion, the error in the Gaussian random numbers induced by the cut-off[1]

[1]It should be mentioned that the output of the Box-Müller algorithm possesses a lower and upper cut-off value of its distribution as well. This limit arises from the random number generator operating on a bounded domain, usually unsigned 32-bit integers. The smallest number uniformly distributed random number is hence $x_{min} = 2^{-32}$. From Eq. (A.23) it then follows for $|y_{\mathrm{BM}}|_{max} = \sqrt{-2\ln(x_{min})} \approx 6.660$.

and the linear interpolation is by far outweighed by the speed of the algorithm.

B Parallel Implementation

This appendix discusses the strategies for implementing the previously discussed algorithms of the noise model, the random number generator and the stochastic partial differential equation in parallel. Parallelized programs allow the simultaneous execution of the numerical simulation on multiple processors of one or separate computers. The benefits of parallelization are the improved performance and the increased amount of available memory[1]. On the downside, we have to take care of causality in the sense that we need to schedule the different processes, so that they run synchronously. Two different architectures have been established for parallelization, the POSIX threads [Nichols et al. 1996] and the Message Passing Interface (MPI) [Snir et al. 1994] libraries.

Pthreads

The traditional approach of using multiple processors, sharing common memory is to create processes that run in parallel on separate processors. A process is defined to contain certain resources, such as an address space together with an user id, file descriptors, directory information and other things necessary for the execution. Moreover, a process is a schedulable unit of execution. These features create a relatively large overhead, which makes it expensive to switch contexts between processes. A thread separates the notion of execution from the notion of resources. A process then defines an address space within which one or more threads can be scheduled independently on the available processors with all threads sharing the common resources of the process. Therefore, threads are light-weight as compared to a process and can be scheduled more efficiently. The POSIX threads programming model revolves around the creation, synchronization and deallocation of threads and managing their execution and the shared resources of the process.

[1] Simulation of a 128×128 network with an integration time of 2^{17} steps uses $\approx 16\,GB$ RAM.

Message Passing Interface

Message passing is often thought of in the context of distributed-memory parallel computers, when the same code can run well on a shared-memory parallel computer. It can run on a network of workstations, or, indeed, as a set of processes running on a single computer. MPI defines standards for the distribution, communication and synchronization of the different parts of the program run in parallel through message passing. Because the different parts do not share common resources in general anymore, the approach towards parallelization of the program needs to be different as compared to the threads model.

Three parts of the total system are suitable to parallelization: the random number generator, the modeling of the noise in space and time and the integration of the spatially extended excitable system.

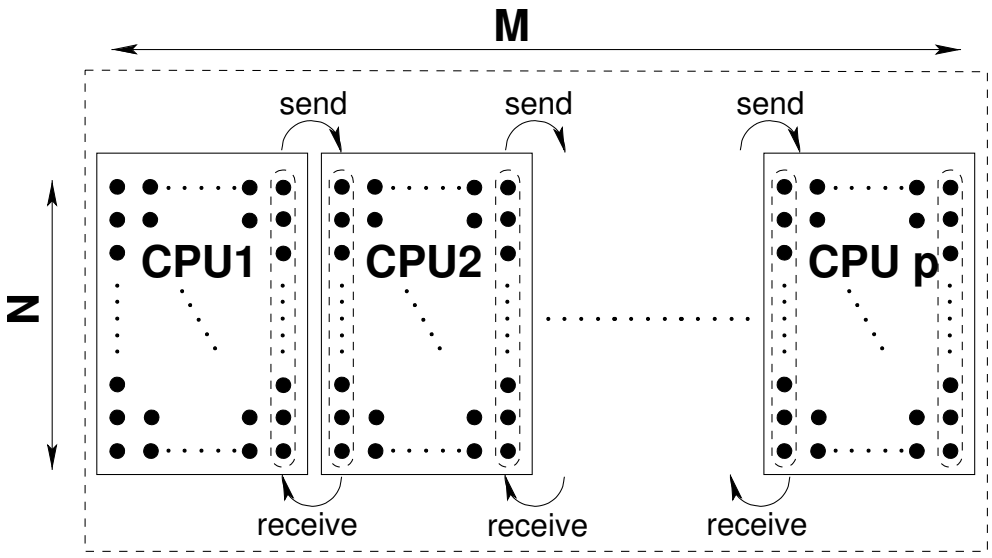

Figure B.1: The parallelization scheme for an the $N \times M$ grid. Each dot stands for a node of the network, therefore each thread iterates a field of size $N \times M/p$. The columns within dotted borders denote those nodes that have to be saved separately in an implementation using distributed memory. The arrows stand for the update calls in an MPI implementation after each integration time step.

B.1 Parallelizing the Network

The simplest parallelization scheme of a two dimensional grid consists in subdividing it into p stripes, where each of the p stripes is handled by a single processor, as shown in Fig. B.1. Care has to be taken to ensure causality amongst the different parts of

the network and the noise field by synchronizing the parallel execution of the network integration and the noise modeling.
Threads use mutual exclusion objects, called mutexes, that allows multiple threads to synchronize access to a shared resource. Once a mutex has been locked by a thread, other threads attempting to lock it will block. This is a way to ensure some global variable is updated sequentially. Each thread performs a certain task, e.g. integrating one time step, and then continues or pauses its execution depending on a global variable that is updated according to the current state of each individual thread. Once all threads have signaled the completion of their tasks, a broadcast message frees all thread locks.
MPI uses a the strategy of blocking and non-blocking calls between the different procedures run in parallel. The latter refers to a one-way communication channel. Some request is sent and the procedures keeps on executing without waiting for a reply. A blocking call signals the current procedure to wait until it has received an answer.
The simulation algorithm is thus iterated with the following steps in a multi-threaded environment

1. spawn p threads and set up the conditional mutex variables for synchronization.
2. allocate the memory for the $N \times M$ field and initialize the network with its initial conditions
3. allocate the diffusion field using the FTCS scheme.
4. initialize the noise
5. iterate the network for one time step in parallel.
6. update the diffusion field values.
7. In the case of a Langevin-type noise in time, update the noise field and apply convolution in space. This can be done in parallel with the use of the multi threaded capabilities of the FFTW algorithm.
8. proceed with the next integration step in (4).

Synchronization calls between threads are made after steps (5–7). This ensures causality both for the noise and the diffusion field .
The MPI implementation uses the same strategy as above, now spawning p processes instead of threads. Nevertheless, the treatment of the diffusive coupling and the noise needs to be different. The distributed memory environment requires to model the

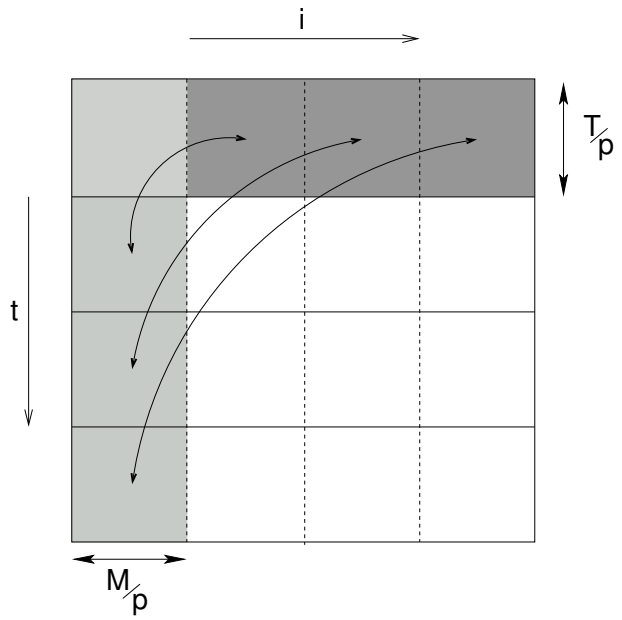

Figure B.2: The memory and pointer swapping scheme for the modeling of the noise. The second spatial dimension is not shown. The dark grey strip shows the first memory chunk used for spatial correlation, the light grey strip is physically located in the same memory area, but contains memory continuous in time after the swapping process.

noise at once with the values of the spatiotemporal noise field distributed to the different memory locations before integration of the SPDEs in time. The overhead of exchanging data for performing the spatial noise convolution at each time step would be too expensive and time consuming. An efficient update scheme regarding the spatial diffusion coupling can be employed with minimal memory redundancy [Zaritski & Pertsov 2002]. Each strip of the network stores the border elements of its respective neighbor strips, which already belong to the next process, in an additional array to be used for calculation of the diffusive coupling (denoted by the grid points within the dotted lines in Fig. B.1). Each process then iterates one integration step in time. After that, the additional border element arrays are updated by two non-blocking send and two blocking receive calls to the left and the right neighbors, respectively. This way, local conditional communication allows for a global synchronization of the whole network.

B.2 Parallelizing the Noise Model

The random number generator can be parallelized by initializing the algorithm separately for each thread or process p.

# Threads	1	2	4	8	16
Thread usage	0.0%	2%	3.8%	7.9%	17%
rel. exec. time	1.0	0.56	0.30	0.16	0.20

Table B.1: Analysis of the multi threaded program efficiency as a function of the number of threads. Thread usage: relative CPU usage of the Pthreads creation, synchronization and deallocation routines with respect to the whole program. Rel. Exec time: the relative execution time as a fraction of the single threaded program. Test were run on an Origin3800, 64GB RAM, 128 CPUs of the URZ TU Dresden

Generating short-range spatiotemporal noise is simple, if considering exponentially correlated noise in time. In this case, the time correlation can be calculated iteratively using an Ornstein-Uhlenbeck process (cf. Sec. 2.3.2), while spatial correlation is ensured by convolving the noise-field with the desired correlation function at each integration step in time.

In the general case of generating the noise by successive convolutions in space and time, one has to use a different approach. The strategy is carried out in a (2 + 1)-dimensional system, but the generalization to higher spatial dimensionality should be straight forward. Having discretized the network onto $N \times M$ grid points in space and integrating over t steps in time, we split the noise field ξ^p_{ijt} first among P processes according to $0 \leq p < P$, $0 \leq j < N$, $0 \leq i < M$ and $T/P * p \leq t < T/P * (p + 1)$, where P should be equal or less than the number or available processors.

Transversing each thread/process memory chunk in time, the grid elements are filled with white noise and convolved accordingly in space. In order to use the noise grid for temporal integration in conjunction with the full SPDE, the memory blocks are then transposed according to Fig. B.2. Now the memory is assigned to the each process according to $0 \leq j < N$, $0 \leq t < T$ and $M/P * p \leq i < M/P * (i + 1)$.

Depending on the memory model used, either shared of distributed memory, the transposition either denotes a simple change in the array indices, or in the latter case, the physical swapping of the memory blocks.

The new memory chunks consist of $M \times N/p \times T$ elements. Transversing all spatial directions, each noise string in time is convolved with the desired temporal correlation function. As a final result, one obtains P memory blocks of spatiotemporally correlated noise values.

Table B.1 is a execution time analysis of the parallelized algorithm using the threads model. The total execution time scales are roughly inverse proportional to the number of threads, less the overhead of the threads and processor idle times, when waiting

for the completion of synchronization calls. The effect of spawning more threads than available processors becomes clear from the last columns. The total execution time then increases instead of decreasing. Multiple threads sharing one processor and are thus slowing down the algorithm. In addition, the CPU idle times increase due to larger latencies of the synchronization calls.
In conclusion, the parallelization scheme presented in this section is not specific to any particular model equation, but can be used for any generic SPDE with an explicit difference scheme, allowing its application to higher dimensions, both for the threads as well as the MPI implementation.

Bibliography

Agladze, K., Keener, J., Müller, S., & Panfilov, A. (1994). "Rotating spiral waves created by geometry". *Science* **264**, 1746–1748.

Alonso, S. & Sagués, F. (2001). "Noise-induced brownian motion of spiral waves". *Phys. Rev. E* **63** 046205, 1–12.

Alonso, S., Sagués, F., & Sancho, J. M. (2002). "Excitability transitions and wave dynamics under spatiotemporal structured noise". *Phys. Rev. E* **65** 066107, 1–11.

Alonso, S., Sendiña-Nadal, I., Pérez-Muñuzuri, V., Sancho, J. M., & Sagués, F. (2001). "Regular wave propagation out of noise in chemical active media". *Phys. Rev. Lett.* **87** 078302, 1–4.

Anishenko, V., Astakhov, V., Neiman, A. B., Vadivasova, T., & Geier, L. S. (2002). *Nonlinear Dynamics of Chaotic and Stochastic Systems*. Springer, Heidelberg.

Aranson, I. S., Chaté, H., & Tang, L.-H. (1998). "Spiral motion in a noisy complex ginzburg-landau equation". *Phys. Rev. Lett.* **80** (12), 2646–2649.

Armero, J., Sancho, M., Casademunt, J., Lacasta, A. M., Ramírez-Piscina, L., & Sagués, F. (1996). "External fluctuations in front propagation". *Phys. Rev. Lett.* **76** (17), 3045–3048.

Bak, P., Tang, C., & Wiesenfeld, K. (1987). "Self-organized criticality: An explanation of the 1/f noise". *Phys. Rev. Lett.* **59**, 381–384.

Ball, P. (1999). *The Self-Made Tapestry*. Oxford University Press.

Barkley, D., Kness, M., & Tuckermann, L. (1990). "Spiral-wave dynamics in a simple model of excitable media: The transition from simple to compound rotation". *Phys. Rev. A* **42**, 2489–2492.

Bartussek, R. (1997). "Ratchets driven by colored gaussian noise". In L. Schimansky-Geier & T. Pöschel (Eds.), *Stochastic Dynamics* (pp. 69–80). Springer, Berlin.

Belousov, B. (1958). In *Referaty po Radiatsionnoi Meditsine za 1945 g (The Abstracts on Radiation Medicine for 1945)* (pp. 145). Medgiz, Moscow.

Benzi, R., Sutera, A., & Vulpiani, A. (1981). "The mechanism of stochastic resonance". *J. Phys. A* **14**, L453–L457.

Bezrukov, S. & Vodyanoy, I. (1997). "Stochastic resonance in non-dynamical systems without response thresholds". *Nature* **385** (6614), 319–321.

Billah, K. Y. R. & Shinozuka, M. (1990). "Numerical method for colored-noise generation and its application to a bistable system". *Phys. Rev. A* **42**, 7492–7495.

Blanter, Y. M. & Büttiker, M. (2000). "Shot noise in mesoscopic conductors". *Physics Reports* **336**, 1–166.

Bronstein, I. & Semendjajew, K. (1989). *Handbuch der Mathematik*. BSB Teubner, Leipzig.

Brunel, N., Chance, F. S., Fourcaud, N., & Abbott, L. F. (2001). "Effects of synaptic noise and filtering on the frequency response of spiking neurons". *Phys. Rev. Lett.* **86** (10), 2186–2189.

Buldú, J. M., García-Ojalvo, J., Mirasso, C. R., Torrent, M. C., & Sancho, J. M. (2001). "Effect of external noise correlation in optical coherence resonance". *Phys. Rev. E* **64** 051109, 1–4.

Bunde, A. & Havlin, S. (1994). *Fractal in Science*. Springer, Heidelberg.

Busch, H., García-Ojalvo, J., & Kaiser, F. (2003). "Pattern formation under the influence of spatiotemporal $1/f^{\alpha}$ noise". *Proceeding of the SPIE* **5114**, 468–477.

Busch, H. & Hütt, M.-T. (2004). "Scale dependence of spatiotemporal filters". *Int. J. Bifur. & Chaos* **14** (6).

Busch, H., Hütt, M.-T., & Kaiser, F. (2001). "Effect of colored noise on networks of nonlinear oscillators". *Phys. Rev. E* **64** 021105, 1–5.

Busch, H., Hütt, M.-T., & Kaiser, F. (2004). "The effect of biological variability on spatiotemporal patterns: model simulations for a network of biochemical oscillators". *Nova Acta Leopoldina* **88**. in press.

Busch, H. & Kaiser, F. (2000). "Noise enhanced signal correlation and wave propagation in networks of oscillatory and excitable systems". *Acta Physica Polonica B* **31** (5), 1143–1156.

Busch, H. & Kaiser, F. (2003). "Influence of spatiotemporally correlated noise on structure formation in excitable media". *Phys. Rev. E* **67** 041105, 1–7.

Bär, M. & Eisenwirth, M. (1993). "Turbulence due to spiral breakup in a continuous excitable medium". *Phys. Rev. E* **48** (3), R1635–R1637.

Cabrera, J. L., Gorroñogoita, J., & de la Rubia, F. (2002). "Coherence enhancement in nonlinear systems subject to multiplicative ornstein-uhlenbeck noise". *Phys. Rev. E* **66** 022101, 1–3.

C++Boost (2003). "Boost c++ libraries". Internet. `http://www.boost.org`.

Chaves, A. (1998). "A fractional diffusion equation to describe lévy flights". *Phys. Lett. A* **239**, 13–16.

Cleveland, W. S., Lin, D., & Sun, D. X. (2000). "IP packet generation: statistical models for TCP start times based on connection-rate superposition". In *Measurement and Modeling of Computer Systems* (pp. 166–177).

Collins, J., Chow, C. C., & Imhoff, T. T. (1995). "Aperiodic stochastic resonance in excitable systems". *Phys. Rev. E* **52**, R3321–R3324.

Compte, A. (1996). "Stochastic foundations of fractional dynamics". *Phys. Rev. E* **53** (4), 4191–4193.

Cross, M. C. & Hohenberg, P. (1993). "Pattern formation outside of equilibrium". *Rev. Mod. Phys.* **65** (3), 851–1112.

Davidenko, J., Pertsov, A. V., Salomonsz, R., Baxter, W., & Jalife, J. (1992). "Stationary and drifting spiral waves of excitation in isolated cardiac muscle". *Nature* **355**, 349–351.

Davies, R. (2000). "Hardware random number generators". `http://www.robertnz.net/hwrng.htm`.

den Broeck, C. V., Parrondo, J., & R.Toral (1994). "Noise-induced nonequilibrium phase transitions". *Phys. Rev. Lett.* **73**, 3395–3398.

Douglass, J., Wilkins, L., Pierson, D., Pantazelou, E., & Moss, F. (1993). "Noise enhancement of information transfer in crayfish mechanoreceptors by stochastic resonance". *Nature* **365**, 337–340.

Dutta, P. (1981). "Low frequency fluctuations in solids: 1/f noise". *Revs. Modern Phys.* **53** (3), 497–516.

Eichenauer-Herrmann, J., Herrmann, E., & Wegenkittl, S. (1997). "A survey of quadratic and inversive congruential pseudorandom numbers". In P. Hellekalek, G. Larcher, H. Niederreiter, & P. Zinterhof (Eds.), *Proceedings of the MC and QMC*, Lecture Notes in Statistics: Springer, New York.

Erneux, T. & Mandel, P. (1986). "Imperfect bifurcation with a slowly-varying control parameter". *SIAM J. Appl. Math.* **46** (1), 1–15.

Fenlason, J. & Stallman, R. (2004). "Gnu gprof - the gnu profiler". `http://www.gnu.org/software/binutils/manual/gprof-2.9.1/`.

Ferrenberg, A. M., Landau, D. P., & Wong, Y. J. (1992). "Monte carlo simulations: Hidden errors from "good" random number generators". *Phys. Rev. Lett.* **69** (23), 3382–3384.

FitzHugh, R. A. (1961). "Impulses and physiological states in theoretical models of nerve membranes". *Biophys. J.* **1**, 445.

Foerster, P., Müller, S., & Hess, B. (1989). "Critical size and curvature of wave formation in an excitable chemical medium". *Proc. Natl. Acad. Sci. USA* **86**, 6831–6834.

Fox, R., Gatland, J., Roy, R., & Vemuri, G. (1988). "Fast, accurate algorithm for numerical simulation of exponentially correlated colored noise". *Phys. Rev. A* **38**, 5938–5940.

Freitag, R. (1999). "Ein zufallszahlengenerator". *Linux Magazin* **6**. `http://www.linux-magazin.de/Artikel/ausgabe/1999/06/Zufallszahlen/zufallszahlen.html`, (in German).

Frigo, M. (1999). "A fast fourier transform compiler". In *Proceedings of the ACM SIGPLAN 1999 conference on Programming language design and implementation* (pp. 169–180).: ACM Press.

Frigo, M. & Johnson, S. (2003). "The fastest fourier transform in the west". Internet. `http://www.fftw.org/`.

Fuliński, A. (1994). "Non-markovian noise". *Phys. Rev. E* **50** (4), 2668–2681.

Gammaitoni, L., Hänggi, P., Jung, P., & Marchesoni, F. (1998). "Stochastic resonance". *Rev. Mod. Phys.* **70** (1), 223–287.

García-Ojalvo, J., Sagués, F., Sancho, J., & Schimansky-Geier, L. (2001). "Noise-enhanced excitability in bistable activator-inhibitor media". *Phys. Rev. E* **65** 011105, 1–6.

García-Ojalvo, J. & Sancho, J. M. (1994). "Colored noise in spatially extended systems". *Phys. Rev. E* **49** (4), 2769–2778.

García-Ojalvo, J. & Sancho, J. M. (1999). *Noise in Spatially Extended Systems*. New York: Springer-Verlag.

García-Ojalvo, J. & Schimansky-Geier, L. (1999). "Noise-induced spiral dynamics in excitable media". *Europhys. Lett.* **47**, 298–303.

Gardiner, C. (1989). *Handbook of stochastic methods*, Vol. 13 of *Springer Series in Physics*. Springer, Berlin, 2nd edition.

Garía-Ojalvo, J., Sancho, J. M., & Ramírez-Picina, L. (1992). "Generation of spatiotemporal colored noise". *Phys. Rev. A* **46** (8), 4670–4675.

Garzik, J. & Rumpf, P. (2000). *The Linux kernel Documentation /usr/src/linux/Documentation/i810_rng.txt*. `http://www.kernel.org/`.

Gerstner, W. & Kistler, W. M. (2002). *Spiking Neuron Models. Single Neurons, Populations, Plasticity*. Cambridge University Press. Available online: `http://diwww.epfl.ch/~gerstner/SPNM/`.

Gingl, Z., Kiss, L., & Moss, F. (1995). "Non-dynamical stochastic resonance: Theory and experiments with white and various coloured noises". *Nuovo Cimento D* **17**, 795–802.

Gluckman, B. J., Netoff, T. I., Neel, E. J., Ditto, W. L., Spano, M. L., & Schiff, S. J. (1996). "Stochastic resonance in a neuronal network from mammalian brain". *Phys. Rev. Lett.* **77** (19), 4098–4101.

Gómez-Gesteira, M., Fernández-Garcìa, G., Muñuzuri, A. P., Pérez-Muñuzuri, V., Krinsky, V. I., Starmer, C. F., & Pérez-Villar, V. (1994). "Vulnerability in an excitable belousov-zhabotinsky medium: From 1d to 2d". *Physica D* **76**, 359–368.

Gray, R. & Jalife, J. (1996). "Sprial waves and the heart". *Int. J. of Bifur. & Chaos* **6** (3), 415–435.

Haahr, M. (1998). "random.org". `http://www.random.org/`.

Haken, H. (1987). *Advanced Synergetics*. Springer, Berlin.

Haussdorff, J. M. & Peng, C.-K. (1996). "Multiscaled randomness: A possible source of 1/f noise in biology". *Phys. Rev. E* **54** (2), 2154–2157.

Hazra, S. N. & Reddy, M. S. (1986). "Design of circularly symmetric low-pass two dimensional fir digital filters using transformation". *IEEE Transactions of Circuits and Systems* **33**, 1022–1026.

Hellekalek, P. (1995). "Inversive pseudorandom number generators: Concepts, results and links". In *Winter Simulation Conference* (pp. 255–262).

Hellekalek, P. (2003). "Random number generators". `http://random.mat.sbg.ac.at/`.

Hempel, H., Schimansky-Geier, L., & García-Ojalvo, J. (1999). "Noise sustained pulsating patterns and global oscillations in subexcitable media". *Phys. Rev. Lett.* **82**, 3713–3716.

Hilfer, R., Ed. (2000). *Applications of Fractional Calculus in Physics*. World Scientific Publishing.

Hilfer, R. & Anton, L. (1995). "Fractional master equation and fractal time random walks". *Phys. Rev. E* **51** (2), R848–R851.

Hodgkin, A. L. & Huxley, A. (1952). "A quantitative description of membrane current and its application to conduction and excitation in nerve". *J. Physiol.* **117**, 500–544.

Honerkamp, J. (1990). *Stochastische Dynamische Systeme*. VCH, Weinheim. (in German).

Horsthemke, W. & Lefever, R. (1984). *Noise-Induced transitions*. Springer Verlag, Berlin.

Hoshen, J. & Kopelman, R. (1976). "Percolation and cluster distribution. i. cluster multiple labeling technique and critical concentration algorithm.". *Phys. Rev. B* **14**, 3438–3443.

Hänggi, P., Jung, P., Zerbe, C., & Moss, F. (1993). "Can colored noise improve stochastic resonance?". *J. Stat. Phys.* **70** (1/2), 25–47.

Hörmann, W. & Leybold, J. (2003). "Continuous random variate generation by fast numerical inversion". *ACM Transaction on Modeling and Computer Simulation* **13** (4), 347–362.

Hütt, M.-T. (2001). *Datenanalyse in der Biologie. Eine Einführung in Methoden der nichtlinearen Dynamik, fraktalen Geometrie und Informationstheorie*. Springer, Berlin.

Hütt, M.-T. & Neff, R. (2001). "Quantification of spatiotemporal phenomena by means of cellular automata techniques". *Physica A* **289**, 498–516.

Hütt, M.-T., Neff, R., Busch, H., & Kaiser, F. (2002). "Method for detecting the signature of noise-induced structures in spatiotemporal data sets". *Phys. Rev. E* **66** 026117, 1–11.

Jensen, H. J. (1998). *Self-Organized Criticality*. Cambridge University Press.

J.S. Nagumo, S. A. & Yoshizawa, S. (1962). "An active pulse transmission line simulating nerve axon". *Proc. IRE* **50**, 2061.

Jung, P. (1997). "Thermal waves, criticality, and self-organization in excitable media". *Phys. Rev. Lett.* **78** (9), 1723–1726.

Jung, P., Cornell-Bell, A. H., Madden, K., & Moss, F. (1998a). "Noise-induced spiral waves in astrocyte syncytia show evidence of self-organized criticality". *J. Neurophys.* **70**, 1098–1101.

Jung, P., Cornell-Bell, A. H., Moss, F., Kádár, S., Wang, J., & Showalter, K. (1998b). "Noise sustained waves in subexcitable media: From chemical waves to brain waves". *Chaos* **8** (3), 567–575.

Jung, P. & Mayer-Kress, G. (1995a). "Noise controlled spiral growth in excitable media". *Chaos* **5**, 459–462.

Jung, P. & Mayer-Kress, G. (1995b). "Spatiotemporal stochastic resonance in excitable media". *Phys. Rev. Lett.* **74**, 2134–2137.

Jähne, B. (1997). *Practical Handbook on Digital Image Processing for Scientific c Applications*. CRC-Press, Boca Raton.

Kádár, S., Wang, J., & Showalter, K. (1998). "Noise supported traveling waves in subexcitable media". *Nature* **391**, 770–772.

Kantz, H. & Schreiber, T. (1997). *Nonlinear time series analysis*. Cambridge University Press.

Karagiannis, T., Faloutsos, M., & Riedi, R. H. (2003). "Long-range dependence: Now you see it, now you don't!". `http://citeseer.nj.nec.com/587746.html`.

Kasdin, N. J. (1995). "Discrete simulation of colored noise and stochastic processes and $1/f^{\alpha}$ power law noise generation". *Proc. IEEE* **83**, 802–827.

Kloeden, P. E. & Platen, E. (1999). *Numerical Solution of Stochastic Differential Equations*. Springer, Berlin.

Knuth, D. E. (1981). *The art of scientific computing, vol. 2: seminumerical algorithms*. Addison-Wesley, Reading.

Kuramoto, Y. (1984). *Chemical Oscillations, Waves, and Turbulence*. Springer-Verlag, Berlin.

Kurrer, C. & Schulten, K. (1991). "Effect of noise and perturbations on limit cycle systems". *Physica D* **50**, 311–320.

Lam, P.-M. & Bagayoko, D. (1993). "Spatiotemporal correlation of colored noise". *Phys. Rev. E* **48** (5), 3267–3270.

Landa, P., Zaikin, A. A., Ushakov, V. G., & Kurths, J. (2000). "Influence of additive noise on transitions in nonlinear systems". *Phys. Rev. E* **61** (5), 4809–4820.

Landa, P. S. & McClintock, P. V. E. (2000). "Changes in the dynamical behaviour of nonlinear systems induced by noise". *Phys. Rep.* **323**, 1–80.

L'Ecuyer, P., Compagner, A., & Cordeau, J. (1996). "Entropy tests for random number generators".

Lee, K. J., Cox, E. C., & Goldstein, R. E. (1996). "Competing patterns of signaling activity in dictyostelium discoideum". *Phys. Rev. Lett.* **76** (7), 1174–1177.

Lee, S.-G., Neiman, A., & Kim, S. (1998). "Coherence resonance in a hodgkin-huxley neuron". *Phys. Rev. E* **57** (3), 3292–3297.

Levin, J. & Miller, J. (1996). "Broadband neural encoding in the cricket sensory system enhanced by stochastic resonance". *Nature* **389**, 165–167.

Lewis, T. & Payne, W. (1973). "Generalized feedback shift register pseudorandom number algorithm". *Journal of the Association for Computing Machinery* **20** (3), 456–468.

Lindner, B., García-Ojalvo, J., Neiman, A., & Schimansky-Geier, L. (2004). "Effects of noise in excitable systems". *Phys. Rep.* **392** (6), 321–424.

Lindner, B. & Schimansky-Geier, L. (1999). "Analytical approach to the stochastic fitzhugh-nagumo system and coherence resonance". *Phys. Rev. E* **60** (6), 7270–7276.

Lindner, J., Meadows, B., Ditto, W., Inchiosa, M., & Bulsara, A. (1995). "Array enhanced stochastic resonance and spatiotemporal synchronization". *Phys. Rev. Lett.* **75**, 3–6.

Ltd., P. T. P. (2004). "The colors of noise". `http://www.msaxon.com/colors.htm`.

Makse, H. A., Havlin, S., Schwartz, M., & Stanley, H. E. (1996). "Method for generating long-range correlations for large systems". *Phys. Rev. E* **53**, 5445–5449.

Mandelbrot, B. (1983). *The Fractal Geometry of Nature*. New York: Freeman.

Mandelbrot, B. B. (1971). "A fast fractional gaussian noise generator". *Water Resources Res.* **7** (3), 543–553.

Marsaglia, G. (1993). "Monkey tests for random number generators". *Computers & Mathematics with Applications* **9**, 1–10.

Marsaglia, G. (2003). "Diehard: a battery of tests for random number generators developed by george marsaglia". `http://stat.fsu.edu/~geo/diehard.html`.

Marsaglia, G. & Zaman, A. (1991). "A new class of random number generators.". *Ann. Appl Prob* **3**, 462–480.

Massanés, S. R. & Vicente, C. J. P. (1999). "Nonadiabatic resonances in a noisy fitzhugh-nagumo neuron model". *Phys. Rev. E* **59** (4), 4490–4497.

Matsumoto, M. (2003). "Mersenne twister: A random number generator". Internet. `http://www.math.keio.ac.jp/~matumoto/emt.html`.

Matsumoto, M. & Kurita, Y. (1992). "Twisted gfsr generators". *ACM Transactions on Modeling and Computer Simulation* **2** (3), 179–194.

Matsumoto, M. & Kurita, Y. (1994). "Twisted gfsr ii". *ACM Transactions on Modeling and Computer Simulation* **4** (3), 254–266.

Matsumoto, M. & Nishimura, T. (1998). "Mersenne twister: A 623-dimensionally equidistributed uniform pseudo-random number generator". *ACM Transactions on Modeling and Computer Simulation* **8** (1), 3–30.

McClellan, J. (1973). "The design of two-dimensional digital filters by transformations". *Proc. of the Annual Princeton Conference on Information Sciences and Systems* **7**, 247–251.

McNamara, B., Wiesenfeld, K., & Roy, R. (1988). "Observation of stochastic resonance in a ring laser". *Phys. Rev. Lett.* **60**, 2626–2629.

Moss, F. & McClintock, P., Eds. (1989). *Noise in Dynamical Systems*. Cambridge University Press, Cambridge.

Muratov, C. & Osipov, V. (1996). "Scenarios of domain pattern formation in a reaction-diffusion system". *Phys. Rev. E* **54** (5), 4860–4879.

Murray, J. (1993). *Mathematical Biology*. Springer, Heidelberg.

Neiman, A., Schimansky-Geier, L., Cornell-Bell, A., & Moss, F. (1999). "Noise-enhanced phase synchronization in excitable media". *Phys. Rev. Lett.* **83** (23), 4896–4899.

Nichols, B., Buttlar, D., & Farrell, J. P. (1996). *Pthreads Programming - A POSIX Standard for Better Multiprocessing*. O'Reily.

Nicolis, G. & Prigogine, I. (1977). *Self-organization in Non-equilibrium Systems, from Dissipative Structures to Order through Fluctuations*. Wiley Interscience, New York.

Niederreiter, H. (1995). "New developments in uniform pseudorandom number and vector generation". In H. Niederreiter & P.-S. Shiue (Eds.), *Monte Carlo and Quasi-Monte Carlo Methods in Scientific Computing, volume 106 of Lecture Notes in Statistics Winter Simulation Conference* (pp. 87–120). Springer, New York.

Nozaki, D., Collins, J., & Yamamoto, Y. (1999a). "Mechanism of stochastic resonance enhancement in neuronal models driven by 1/f noise". *Phys. Rev. E* **60**, 4637–4644.

Nozaki, D., Mar, D. J., Grigg, P., & Collins, J. J. (1999b). "Effects of colored noise on stochastic resonance in sensory neurons". *Phys. Rev. Lett.* **82** (11), 2402–2405.

Nozaki, D. & Yamamoto, Y. (1998). "Enhancement of stochastic resonance in a fitzhugh-nagumo neuronal model driven by colored noise". *Phys. Lett. A* **243**, 281–287.

Nozakura, T. & Ikeuchi, S. (1984). "Formation of dissipative structures in galaxies". *Astr. J.* **279**, 40–52.

Osborne, A. R. & Provenzale, A. (1989). "Finite correlation dimension for stochastic systems with power-law spectra". *Physica D* **35**, 357–381.

Ouyang, H. F. & Huang, Z. Q. (1994). "1/f noise and one-dimensional brownian motion in a singular potential". *Phys. Rev. E* **50** (4), 2491–2496.

Paczuski, M., Maslov, S., & Bak, P. (1996). "Avalanche dynamics in evolution, growth, and depinning models". *Phys. Rev. E* **53** (1), 414–443.

Parrondo, J. & de Cisneros, B. (2002). "Energetics of brownian motors: a review". *Appl. Phys. A* **75**, 179–191.

Peng, C.-K., Hausdorff, J. M., & Goldberger, A. L. (2000). "Fractal mechanisms in neuronal control: human heartbeat and gait dynamics in health and disease". In J. Walleczek (Ed.), *Self-Organized Biological Dynamics & Nonlinear Control*. Cambridge University Press.

Pérez-Muñuzuri, V., Sagués, F., & Sancho, J. M. (2000). "Lifetime enhancement of scroll rings by spatiotemporal fluctuations". *Phys. Rev. E* **62**, 94–99.

Petrov, V., Ouyang, Q., & Swinney, H. L. (1997). "Resonant pattern formation in a chemical system". *Nature* **388**, 655–657.

Pikovsky, A. & Kurths, J. (1997). "Coherence resonance in a noise-driven excitable system". *Phys. Rev. Lett.* **78**, 775–778.

Pikovsky, A., Rosenblum, M., & Kurths, J. (2001). *Synchronization: a universal concept in nonlinear sciences*. Cambridge University Press.

Prakash, S., Havlin, S., Schwartz, M., & Stanley, H. E. (1992). "Structural and dynamical properties of long-range correlated percolation". *Phys. Rev. A* **46** (4), R1724–R1727.

Press, W. H., Teukolsky, S. A., Vetterling, W. T., & Flannery, B. P. (1993). *Numerical Recipes in C, 2nd Edition*. Cambridge University Press, New York.

Ramírez-Picina, L., Sancho, J., & Hérnandez-Machado, A. (1993). "Numerical algorithm for ginzburg-landau equations with multiplicative noise: Application to domain growth". *Phys. Rev. B* **48** (1), 125–131.

Rascher, U., Hütt, M.-T., Siebke, K., Osmond, B., Beck, F., & Lüttge, U. (2001). "Spatio-temporal variation of metabolism in a plant circadian rhythm: the biological clock as an assembly of coupled individual oscillators". *Proc. Natl. Acad. Sc. USA* **98** (20), 11801–11805.

Richardson, K., Imhoff, T., Grigg, P., & Collins, J. (1998). "Using electrical noise to enhance the ability of humans to detect subthreshold mechanical cutaneous stimuli". *Chaos* **8**, 599–603.

Risken (1984). *The Fokker-Planck Equation*. Springer, Heidelberg.

Rogers, T., Elder, K., & Desai, R. C. (1988). "Numerical study of the late stages of spinodal decomposition". *Phys. Rev. B* **37** (16), 9638–9649.

Russell, D. F., Wilkens, L. A., & Moss, F. (1999). "Use of behavioural stochastic resonance by paddle fish for feeding". *Nature* **402**, 291–294.

Saletti, R. (1986). "A comparison between two methods to generate $1/f^{\gamma}$ noise". *Proc. IEEE* **74**, 1595–1596.

Sandfuchs, O., Kaiser, F., & Belić, M. R. (2001). "Self-organization and fourier selection of optical patterns in a nonlinear photorefractive feedback system". *Phys. Rev. A* **64** 063809, 1–20.

Saul, A. & Showalter, K. (1985). "Propagating reaction-diffusion fronts". In R. J. Field & M. Burger (Eds.), *Oscillations and Traveling waves in Chemical Systems*. Wiley & Sons.

Schreiber, T. (2000). "Measuring information transfer". *Phys. Rev. Lett.* **85** (2), 461–464.

Schulten, K. & Kosztin, I. (2000). "Lectures in theoretical biophysics". `http://www.ks.uiuc.edu/Services/Class/NSM.pdf`, U. of Illinois, Illinois, USA.

Scinicariello, A., Eaton, K., Inglis, J., & Collins, J. (2001). "Enhancing human balance control with galvanic vestibular stimulation". *Biological Cybernetics* **84**, 475–480.

Sendiña-Nadal, I., Alonso, S., Perez-Muñuzuri, V., Gómez-Gesteira, M., Pérez-Villar, V., Ramírez-Picina, L., Casademut, J., Sancho, J. M., & Sagués, F. (2000). "Brownian motion of spiral waves driven by spatiotemporal structured noise". *Phys. Rev. Lett.* **84**, 2734–2737.

Sendiña-Nadal, I., Muñuzuri, A., Vives, D., Perez-Muñuzuri, V., Casademut, J., Ramírez-Picina, L., Sancho, J. M., & Sagués, F. (1998a). "Wave propagation in a medium with disordered excitability". *Phys. Rev. Lett.* **80**, 5437–5440.

Sendiña-Nadal, I. & Pérez-Muñuzuri (2001). "Noise-enhanced wave train propagation in unexcitable media". *Int. J. Bifur. & Chaos* **11**, 2837–2843.

Sendiña-Nadal, I., Roncaglia, D., Vives, D., Pérez-Muñuzuri, V., Gómez-Gesteira, M., Pérez-Villar, V., Echave, J., Casademunt, J., Ramírez-Piscina, L., & Sagués, F. (1998b). "Percolation thresholds in chemical disordered excitable media". *Phys. Rev. E* **58** (2), R1183–R1186.

Sethna, J. P., Dahmen, K. A., & Myers, C. R. (2001). "Crackling noise". *Nature* **430** (8), 242–250.

Shannon, C. (1948). "A mathematical theory of communication". *Bell Syst. Techn. J.* **27**, 379–423.

Shulgin, B., Neiman, A., & Anishchenko, V. (1995). "Mean switching frequency locking in stochastic bistable systems driven by a periodic force". *Phys. Rev. Lett.* **75** (23), 4157–4160.

Snir, M., Otto, S., Huss-Lederman, S., Walker, D., & Dongarra, J. (1994). *MPI, The Complete Reference*. MIT Press. Avail. Online: `http://www.netlib.org/utk/papers/mpi-book/node1.html`.

Stanley, H. E., Amaral, L. A. N., Buldyrev, S. V., Gopikrishnan, P., Plerou, V., & Salinger, M. A. (2002). "Self-organized complexity in economics and finance". *Proc. Natl. Acad. Sc. USA* **99**, 2561–2565.

Stauffer, D. & Aharony, A. (1994). *Introduction to Percolation Theory*. Taylor and Francis, London, 2nd edition.

Steinbock, O., Kettunen, P., & Showalter, K. (1995). "Anisotropy and spiral organizing centers in patterned excitable media". *Science* **269**, 1857–1860.

Steinbock, O., Zykov, V., & Müller, S. (1993). "Control of spiral-wave synamics in active media by periodic modulation of excitability". *Nature* **366**, 322–324.

Stocks, N. (2000). "Suprathreshold stochastic resonance in multilevel threshold systems". *Phys. Rev. Lett.* **84** (11), 2310–2313.

Toral, R. & Chankrabarti, A. (1993). "Generation of gaussian distributed random numbers by using a numerical inversion method". *Comp. Phys. Commun.* **74**, 327–334.

Ts'o, T. (1999). *The Linux kernel Documentation /usr/src/linux/drivers/char/random.c*. `http://www.kernel.org/`.

Turing, A. (1952). "The chemical basis of morphogenesis". *Phil. Trans. R. Soc. London B* **237**, 37–72.

Tyson, J. & Keener, J. (1988). "Singular perturbation theory of traveling waves in excitable media". *Physica D* **32**, 327–361.

van Kampen, N. (2001). "Foreword: the theory of noise". *Fluc. And Noise Lett.* **1** (1), 3–7.

van Kampen, N. G. (1992). *Stochastic Processes in Physics and Chemistry*. Elsevier Science Publishers, B.V., Amsterdam.

Wagner, R. (2003). "Mersenne twister c++ class". Internet. `http://www.personal.engin.umich.edu/~wagnerr/MersenneTwister.html`.

Wang, J., Kádár, S., Jung, P., & Showalter, K. (1999). "Noise driven avalanche behavior in subexcitable media". *Phys. Rev. Lett.* **82**, 855–858.

Willinger, W., Paxon, V., Reidi, R., & Taqqu, M. (2001). "Long-range dependence and data network traffic". In G. O. P. Doukhan & M. S. Taqqu (Eds.), *Long-range Dependence: Theory and Applications*. Birkhäuser.

Winfree, A. T. (1972). "Spiral waves of chemical activity". *Science* **175**, 634–635.

Winfree, A. T. (1980). *The Geometry of Time*. Springer, New York.

Winfree, A. T. (1991). "Varieties of spiral wave behavior: An experimentalist's approach to the theory of excitable media". *Chaos* **1**, 303–334.

Wornell, G. W. (1990). "A karhunen-loeve-like expansion for 1/f processes via wavelets". *IEEE Trans. on Info. Theory* **36**, 859–861.

Wornell, G. W. (1993). "Wavelet-based representations for the 1/f family of fractal processes". *Proc. IEEE* **810**, 1428–1450.

Yamada, S., Nakashima, M., Matsumoto, K., & Shiono, S. (1993). "Information theoretic analysis of action potential trains i. analysis of correlation between two neurons". *Biol. Cybern.* **68**, 215–220.

Yamada, S., Nakashima, M., Matsumoto, K., & Shiono, S. (1996). "Information theoretic analysis of action potential trains ii. analysis of correlation among n neurons to deduce connection structure". *J. Neurosci. Methods.* **66**, 35–45.

Zaikin, A. (2003). "Noise-induced transitions and resonant effects in nonlinear systems". http://pub.ub.uni-potsdam.de/2003/0017/zaikin.pdf. Habil.-Schr., Potsdam Univ.

Zaikin, A. & Schimansky-Geier, L. (1998). "Spatial patterns induced by additive noise". *Phys. Rev. E* **58** (4), 4355–4360.

Zaikin, A. N. & Zhabotinsky, A. M. (1970). "Concentration, wave propagation in two-dimensional liquid-phase self-organizing system". *Nature* **255**, 535–536.

Zaritski, R. M. & Pertsov, A. M. (2002). "Simulation of 2-d spiral wave interactions on a pentium-based cluster."". In M. P. Bekakos, G. S. Ladde, N. G. Medhin, & M. Sambandham (Eds.), *Proceedings of Neural, Parallel, and Scientific Computations*, Vol. 2 (pp. 187–190).: Dynamic Publishers.

Zhang, L. & Seaton, N. (1992). "Prediction of the effective diffusivity in pore networks close to a percolation threshold.". *AIChEJ* **38** (11), 1816–1824.

Zhonghuai, H., Lingfa, Y., Zuo, X., & Houwen, X. (1998). "Noise induced pattern transition and spatiotemporal stochastic resonance". *Phys. Rev. Lett.* **81**, 2854–2857.

Zhou, Y. & Jung, P. (2000). "Noise and complexity in three dimensional excitable media". *Europhys. Lett.* **49**, 695–701.

Acknowledgments

I would like to thank Prof. Dr. Friedemann Kaiser for his warm reception in his group, giving me the possibility to carry out this research. His precise criticism and keen insight into the field of non-linear dynamics, his freedom and trust granted to the members of his group are valuable qualities hard to find.
Prof. Dr. Marc-Thorsten Hütt deserves thanks for his valuable hours of time shared for discussion, his enthusiasm and urge to pursue and push new ideas, which has led to a fruitful collaboration. Especially his splendid introduction to country and western music while driving down the long roads in the South Western USA deserves notion.
I want to express my gratitude for being given the opportunity to collaborate with other scientists in the Graduiertenkolleg 340. As an associate member I was fortunate to gain some insight into the highly complex, noisy and interesting field of Biology and to exchange views on noise and physics and living matter in the Biology Department as well as on conferences throughout the world.
I would like to extend my thanks to Prof. Jordi García-Ovalvo for his warm reception in his group in Barcelona, Spain, granting me access to the computer systems to carry out some of the numerical investigations.
I also want to mention Andreas Deutsch, who was so kind to offer to me some of their computer resources at their facility, the URZ in Dresden.
Not many people share the luck to work together with these splendid characters and unique people that once made or still make up the Nonlinear Dynamics Groups. In particular, Andreas Stepken, Ivona 'Zerajic'and Kristian Motzek. Not forgetting - of course - Andreas Bohn, remembering him for our intuitive mutual, verbal and non-verbal understanding. A special thanks goes out to Kristian Motzek for the critical review of the manuscript.
All along the list is my used-to-be home, the ever inspiring Karlshof and my former flat mates and neighbors there. René deserves notion for his interest in my work and his never fading will to read my manuscript.
A special thanks goes out to my relatives and in particular to my parents for all the support and patience during all those years.
Last not least, a big, big thank you to my beloved wife Sabine. This work would not have been possible without her. Her patience and loving care carried my through times of hardship and kept up my endurance.

Summary

Pattern formation and synchronization in spatially extended systems are a central topic of ongoing research in many fields of science. The omnipresence of noise in natural systems is a fact that has led to controversial discussions over the last decades, the question being whether natural system actively make use of ambient fluctuations in synchronization or pattern forming processes. One possibility for a system to make use of noise in a constructive way is the notion of Stochastic Resonance, a phenomenon wherein the signal processing capabilities of a system are optimized under the influence of a moderate noise level. The idea of noise being beneficial to the system dynamics has been extended to spatially extended media, called Spatiotemporal Stochastic Resonance, in which noise induces and/or sustains spatiotemporal patterns. The existence of Stochastic Resonance in purely temporal and spatially extended systems has ever since been confirmed in many experiments in physics, chemistry and biology.
Noise in natural systems usually has finite spatiotemporal correlations, noise is then said to be 'colored'. With the eye on biological systems, it is thus important to investigate the influence of these noise correlations on the effect of Spatiotemporal Stochastic Resonance and synchronization in excitable and oscillatory media, respectively.
The aim of this thesis is thus threefold. Numerical algorithms for the efficient modeling of spatiotemporal correlated noise are developed and tested. Different analysis tools for the detection and extraction of coherent structures from a noisy, spatially extended system are introduced and evaluated, which deduce the global state of the system from the local dynamics in a cellular-automaton fashion. These tools are finally used to investigate the effect of additive, spatiotemporal correlated noise on a two dimensional network of biologically motivated elements, in its respective noise-sustained pattern forming, its excitable and its oscillatory regime. We perform the investigations separately for two different noise types, which are commonly encountered in natural systems. The first type shows short-range, exponentially decaying correlations both in time and space, whereas the second type has long-range spatiotemporal correlations. It is also called power-law noise due to its specific power-law shape of the spatiotemporal spectral energy distribution.

The spatiotemporal noise is simulated by Fourier filtering a white, i.e. uncorrelated, noise field with an appropriate FIR filter. The network is integrated using a Heun method in time and an explicit stepping scheme in space.
In summary, the results of this thesis lead to the following conclusions:

- Noise-induced pattern formation is a robust phenomenon with respect to a wide range of spatiotemporal noise correlations. Indeed, a moderate temporal noise correlation is beneficial to the effect of Spatiotemporal Stochastic Resonance for both short- and long-range correlated noise. This optimization at intermediate noise color also holds true for the spatial noise correlation in the case of power-law noise. The effect is attributed to the self-affine properties of this particular type of noise. Short-range correlated noise lacks multi-scale properties, and one thus finds a monotonous shift of the optimal noise intensity for pattern formation towards smaller noise levels with increasing spatial noise color.

- Data analysis confirms that spatiotemporal colored noise enhances the pattern forming process in excitable media as well by inducing 'turbulent', yet, in relation to the system size, large structures in the medium.

- The effect of spatial desynchronization or inhomogeneity in an oscillatory system is enhanced by both intermediate short- and long-range correlated noise for moderate temporal and spatial noise color.

- The location of the maximal system-inhomogeneity with respect to temporal noise correlation changes with the system parameters of the individual oscillators and is directly related to their limit cycle frequency. This location remains unaffected from the system parameters with respect to spatial noise color, but it depends on the system size instead.

- The above findings are reproduced analytically by a linear response analysis, which views the respective media in terms of their spatiotemporal frequency filter characteristics. The results are in good agreement with the simulations for any temporally correlated noise, but generally disagree for large spatial noise color due to finite size effects of the system. The analysis shows that the influence of colored noise on the pattern forming and synchronization processes is a consequence of the impact of the noise color on the energy transfer from the noise to the medium by changing the noise's power spectral density, and thus its correlation with the frequency response of the system.

- The analytical results deviate from the numerical simulations in the case of spatial power-law noise not only due to finite-size effects, but also due to the particular self-affine properties of the noise, which the theory does not account for.

Altogether, the results put the phenomenon of Spatiotemporal Stochastic Resonance on a broader theoretical and numerical footing. Its robustness to spatiotemporal noise color makes this effect a candidate for noise-induced phenomena in nature. It is to be expected, that noise in neuro-physiological systems can have indeed favorable effects.

Zusammenfassung

Strukturbildung und Synchronisation in räumlich ausgedehnten Systemen sind ein Gebiet aktueller Forschung in vielen Disziplinen der Wissenschaft. Rauschen und Fluktuationen sind in der Natur allgegenwärtig. In den letzten Jahren is deshalb eine kontroverse Diskussion darüber ausgebrochen, ob reale Systeme das sie beeinflussende Rauschen aktiv zur Signalverarbeitung, gegenseitiger Synchronisation oder Musterbildung nutzen. Eine theoretische Möglichkeit, wie Rauschen in einem konstruktiven Sinn genutzt werden kann, ist das Phänomen der Stochastischen Resonanz. Diese beschreibt, wie ein System die Kohärenz oder Verstärkung zwischen Eingangs- und Ausgangssignal bei einer mittleren Rauschstärke optimieren kann. Die Idee, Rauschen aktiv zu nutzen, wurde auf räumlich ausgedehnte Systeme erweitert und wird Raumzeitliche Stochastische Resonanz genannt. Hier wird die Energie des raumzeitlich fluktuierenden Treibers zur Bildung kohärenter, geordneter Muster genutzt. Seit ihrer theoretischen Formulierung ist die Existenz von Stochastischer Resonanz in diversen Experimenten mit rein zeitlichen, aber auch räumlich ausgedehnten Systemen der Physik, Biologie und Chemie nachgewiesen worden.
Rauschen in der Natur zeigt für gewöhnlich finite raumzeitliche Korrelationen, man sagt auch, das Rauschen sei 'farbig'. Aus diesem Grund ist es in Hinblick auf biologische Systeme wichtig zu untersuchen, welchen Einfluß eine Änderung der Rauschfarbe auf rauschinduzierte Musterbildung und Synchronisation in exzitatorischen und oszillatorischen Medien hat.
Die Ziele dieser Arbeit gestalten sich deshalb wie folgt: wir entwickeln und testen effiziente numerische Algorithmen zur Simulation raumzeitlichen Rauschens. Wir stellen verschiedene Methoden zur Detektion und Quantifizierung kohärenter Strukturen in raumzeitlichen, verrauschten Datensätzen vor. Die Methoden quantifizieren eine mittlere Kohärenz des gesamten Systems, ähnlich einem zellulären Automaten, aus der Betrachtung von Netzwerknachbarschaften. Diese Werkzeuge werden sodann genutzt, um den Einfluß von additivem, raumzeitlich korreliertem Rauschen auf ein zweidimensionales Netzwerk, bestehend aus biologisch motivierbaren FitzHugh-Nagumo Systemen, auf Strukturbildung und Synchronisationeseigenschaften hin zu

untersuchen. Die Untersuchungen geschehen separat für zwei verschiedenen Rauscharten, die beide in reellen Systemen anzutreffen sind. Der erste Typ besitzt kurzreichweitige, exponentiell abfallende Korrelationen in Raum und Zeit, wohingegen der zweite Rauschtyp durch seine langreichweitigen Korrelationen charakterisiert ist. Dieser Typ wird auch Power-Law Rauschen genannt, da seine spektrale, raumzeitliche Energieverteilung in der Form eines Potenzgesetzes abfällt.
In dieser Arbeit wird das raumzeitlich korrelierte Rauschen mit Hilfe der Fourier Filterung erzeugt, indem weißes, d.h. unkorreliertes, Rauschen mit einem entsprechenden Frequenzfilter gefaltet wird. Das Netz aus gekoppelten, stochastischen Differentialgleichungen wird mittels der Heun Methode in der Zeit und durch ein explizites Schrittverfahren im Raum integriert.
Zusammenfassend kommen die Untersuchungen dieser Arbeit zu den folgenden Ergebnissen:

- Rauschinduzierte Strukturbildung ist robust gegenüber einem großen Bereich raumzeitlicher Rauschkorrelationen. Eine mittlere zeitliche Korrelationslänge optimiert den Effekt der Raumzeitlichen Stochastischen Resonanz sowohl für kurz- als auch für langreichweitiges Rauschen. Im Falle von Power-Law Rauschen wird dieser Effekt ebenso für eine mittlere räumliche Korrelationslänge optimiert. Der Grund dafür liegt in der Selbstähnlichkeit dieses Rauschens. Exponentiell korreliertes Rauschen hingegen besitzt dieses Multiskalenverhalten nicht. Deshalb verlagert sich die Rauschstärke für optimale Strukturbildung mit wachsender räumlicher Rauschfarbe monoton zu kleineren Rauschintensitäten.

- Die Datenanalyse zeigt, daß raumzeitliches, farbiges Rauschen die Strukturbildung in exzitatorischen Medien ebenso verbessern kann, indem es 'turbulente', aber dennoch im Vergleich zur Systemgröße große Strukturen erzeugt.

- Amplitudendesynchronisation oder Inhomogenität in einem oszillierenden Medium wird sowohl von einer mittleren räumlichen, als auch zeitlichen Rauschfarbe maximiert. Der Effekt ist qualitativ unabhängig vom gewählten Rauschtyp.

- Die Position der maximalen Inhomogenität in bezug auf die zeitliche Rauschkorrelation verschiebt sich mit Änderung der einzelnen Oszillatorparameter und ist direkt mit der Grenzzyklusfrequenz verknüpft. Die Position der maximalen Inhomogenität in Hinblick auf die räumliche Korrelationslänge hingegen ist einzig von der Systemgröße abhängig.

- Die oben genannten numerischen Ergebnisse können analytisch mittels einer linearen Antworttheorie bestätigt werden. Diese abstrahiert das exzitatorische und

oszillierende Medium unter dem Aspekt ihrer raumzeitlichen Frequenzfiltereigenschaften. Aus der Theorie geht hervor, daß sich die obigen Effekte des raumzeitlich korrelierten Rauschens auf die Strukturbildung und Synchronisation aus dem Einfluß der Rauschfarbe auf den Energieübertrag des Rauschens auf das System erklären lassen. Diese raumzeitlichen Korrelationen verändern das Frequenzspektrum des Rauschens und somit die Korrelation mit der Frequenzverstärkung des Systems.

- Die lineare Antworttheorie stimmt im Allgemeinen gut mit den numerischen Simulationen überein. Dennoch gibt es Abweichungen auf Grund der endlichen Größe des untersuchten Systems und besonders im Fall des räumlich korrelierten Power-Law Rauschens, da die Theorie nicht für die Betrachtung selbstähnlicher Prozesse ausgelegt ist.

Abschließend läßt sich sagen, daß die hier gewonnenen Ergebnisse das Phänomen der Raumzeitlichen Stochastischen Resonanz auf ein breiteres numerisches, und auch theoretisches Fundament stellen. Durch seine Robustheit gegenüber raumzeitlich korreliertem Rauschen könnte dieser Effekt durchaus in verschiedenen physikalischen, biologischen und chemischen Systemen eine Rolle spielen.

Curriculum Vitae

Personal Data

Name	Hauke Stephan Busch
Date of Birth	7.2.1972
Place of Birth	Aschaffenburg
Nationality	German
Status	married
Address	Kranichsteiner Straße 11, 64289 Darmstadt, Germany

School Education

1978–1982	Don-Bosco-Schule Künzell, Grundschule
1982–1992	Freiherr-vom-Stein-Schule Fulda, Gymnasium
1989–1990	Exchange student at the Cranston HighSchool West, RI, USA
6/1990	American High School Diploma
6/1992	Abitur

Higher Education

1992–1998	Study in Physics at the Darmstadt University of Technology
1995–1996	EU-SOCRATES exchange year at the Trinity College, Dublin
1997–1998	Diplomarbeit (Dissertation), supervisor: Prof. Dr. F. Kaiser Inst. of Applied Physics, Darmstadt University of Technology Title: 'Signal correlation in coupled excitable Oscillators'.
12/1998	Diplom-Physiker (eqiv. M.Sc)
4/1999–3/2004	PhD thesis, supervisor: Prof. Dr. F. Kaiser, Inst. of Applied Physics, Physics Department, Darmstadt University of Technology.
4/1999–4/2002	Associate Member of the DFG Graduiertenkolleg 340 'Communication in Biological Systems'.
9/2002–11/2002	Short visit to the UPC, Barcelona, Spain.

"So long and thanks for all the fich."

DOUGLAS ADAMS

Hiermit erkläre ich an Eides Statt, dass ich
die vorliegende Dissertation selbständig verfasst
und nur die angegebenen Hilfsmittel verwendet habe.
Ich habe bisher keinen Versuch unternommen, an einer
anderen Hochschule das Promotionsverfahren einzuleiten.

Darmstadt, im April 2004